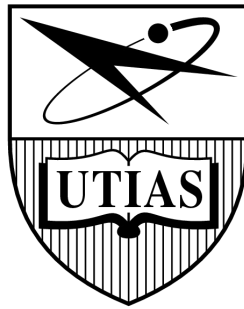# Statistical Arbitrage with Limit Order Book Imbalance

Anton Rubisov

University of Toronto Institute for Aerospace Studies

Faculty of Applied Science and Engineering

University of Toronto

A thesis submitted in conformity with the requirements

for the degree of *Master of Applied Science*

Statistical Arbitrage with
Limit Order Book Imbalance

Anton Rubisov

University of Toronto Institute for Aerospace Studies
Faculty of Applied Science and Engineering
University of Toronto

2015

Abstract

This dissertation demonstrates that there is high revenue potential in using limit order book imbalance as a state variable in an algorithmic trading strategy. Beginning with the hypothesis that imbalance of bid/ask order volumes is an indicator for future price changes, exploratory data analysis suggests that modelling the joint distribution of imbalance and observed price changes as a continuous-time Markov chain presents a monetizable opportunity. The arbitrage problem is then formalized mathematically as a stochastic optimal control problem using limit orders and market orders with the aim of maximizing terminal wealth. The problem is solved in both continuous and discrete time using the dynamic programming principle, which produces both conditions for market order execution, as well as limit order posting depths, as functions of time, inventory, and imbalance. The optimal controls are calibrated and backtested on historical NASDAQ ITCH data, which produces consistent and substantial revenue.

Acknowledgements

And I would like to acknowledge ...

Contents

List of Figures

List of Tables

List of Corrections

Chapter 1

Introduction

With the introduction of mathematical models, participation in financial markets evolved from an art to a science. Beginning with Harry Markowitz's modern portfolio theory, moving through the capital asset pricing model and the Black-Scholes option pricing model, modern finance is now replete with models for pricing derivatives, credit scores, and costs of capital; what was once speculation is now calculation. Crucially, models lead to algorithms, which remove human error and add the ability to process large sets of data.

The process of running computer algorithms to execute orders on an electronic exchange such as NASDAQ is known as *algorithmic trading*. Speed of execution is typically paramount, often requiring running the algorithms on servers directly wired to the exchange, known as *co-location*. Closely related is *high-frequency trading*, which refers simply to the timescale, generally milliseconds, on which the algorithms submit orders. In theory, high-frequency trading is encompassed by algorithmic trading, while not all algorithmic trading need be high-frequency; in practice, the two terms are often used interchangeably.

The particular algorithms used in algorthmic trading vary greatly across the different types of strategies employed. Non-revenue-generating algorithmic trading is generally aimed at transaction cost reduction, with the primary theoretical paper on the subject being Bertsimas and Lo (1998) and Almgren and Chriss (2001). When an institutional investor wishes to buy or sell a large quantity of shares, the aim of the trader is to obtain the best possible price compared with some benchmark (often taken to be the midprice at the time of initiating the strategy). Here the definition of 'large' is determined relative to the liquidity of the stock - either in comparison to the average size of trades for the

given stock, or to the available quantity to be bought/sold at the best listed price. The goal of the algorithmic trading strategy is then to split the large order into smaller pieces and execute them on an algorithmically-determined schedule, balancing the total time for execution with the volatility of the price the trader will receive.

Conversely, an example of algorithmic trading that capitalises on arbitrage opportunities to generate revenue is cross-exchange arbitrage, which uses simple, low-latency algorithms to profit from price discrepancies of a single stock dual-listed on two exchanges. The server running the algorithm is co-located at one of the exchanges, algorithm latency is on the order of microseconds, and the limiting reagent is the time taken for information to travel to and from the other exchange. In the case of Chicago and New York, for example, information can make the trip in 6ms via optical fibres that send information at about half the speed of light. For this reason, agents are now paying for access to a system of ground satellites that has been set up to relay information between the two exchanges via microwaves, shaving latency down to 4ms (Laughlin et al., 2014). Another class of strategies for generating revenue using algorithmic trading are statistical arbitrage strategies, which use complex algorithms to profit from observed statistical patterns of a single stock on a single exchange. In statistical arbitrage, the aim is to exploit predictable statistical patterns in the available data provided by the exchange, such as predicting stock price movements from prices observed thus far. This method too requires co-location, and operates on the scale of milliseconds. It is this type of high-frequency trading that is explored in this dissertation.

As part of the Dodd-Frank Act of 2010, the Volcker Rule has banned US banks from making certain speculative investments, and in so doing effectively curbed their proprietary high frequency trading activity. Nevertheless, as they are still required to provide liquidity to markets via market-making (offering to both buy and sell financial instruments), banks use algorithmic trading to determine the bid/ask bands they will send to exchanges. Exploiting arbitrage opportunities using high frequency trading remains unrestricted for hedge funds, and notably has been used by Renaissance Technologies LLC's flagship Medallion fund to generate an average 71.8 percent annual return, before fees, from 1994 through mid-2014 (Rubin and Collins, 2015). However, as it remains exclusive to only Renaissance employees and family members, it serves instead as a reminder of the revenue potential of high frequency algorithmic trading.

1.1 The Limit Order Book

A *limit order* is an instruction submitted by an agent to buy or sell up to a specified quantity or volume of a financial instrument, and at a specified price. A *limit order book (LOB)* is the accumulated list of such orders sent to a given exchange, where each order is accompanied by a timestamp and an anonymous key that uniquely identifies the agent. The exchange runs a trade matching engine that uses the LOB to pair buy and sell requests that concur on price, even if only partially on volume. Orders remain in effect until they are modified, cancelled, or fully filled (Kyle, 1989).

The unfilled or partially filled orders accumulate in the limit order book and provide liquidity to the market. At any given time, the structure of the LOB can be visualised as in Figure 1.1. As new limit orders arrive, they are compared with existing opposing orders in the book in search of a match - and if so, existing orders are *filled* or *lifted* according to a first-in-first-out priority queue for each price level. The price levels can also be referred to by their *depth*, where the best bid and ask prices are called *at-the-touch* and have a depth of zero, and depth increases in either direction according to the absolute price difference from the at-the-touch depths; the buy limit order at \$28.92 is at a depth of \$0.02. *Market orders* extend the idea of limit orders by specifying only the volume, and accept the best possible price currently available in the LOB; whereas limit orders are free to post, modify, and cancel (as an incentive for providing liquidity), a fee is charged for executing a market order.

In the literature, LOBs are generally modelled in one of two ways: either by an economics-based approach, or a physics-based approach (Gould et al., 2013). The economics-based approaches are trader-centric, assume perfect rationality, view order flow as static, and seek to understand trader strategies, in particular through game-style theories. By contrast, the physics-based approach, with which we are more concerned here, assumes zero-intelligence, provides conceptual toy models of the evolution of the book, and is concerned with the search for statistical regularity. The dynamics of the book, namely order arrivals and cancellations, are governed by stochastic processes of varying complexity, from particles on a 1-D price lattice (Bak et al., 1997) to independent Poisson processes governing the arrival, modification, and cancellation of orders (Cont et al., 2010). An excellent literature survey on LOB modelling can be found in Gould et al. (2013).
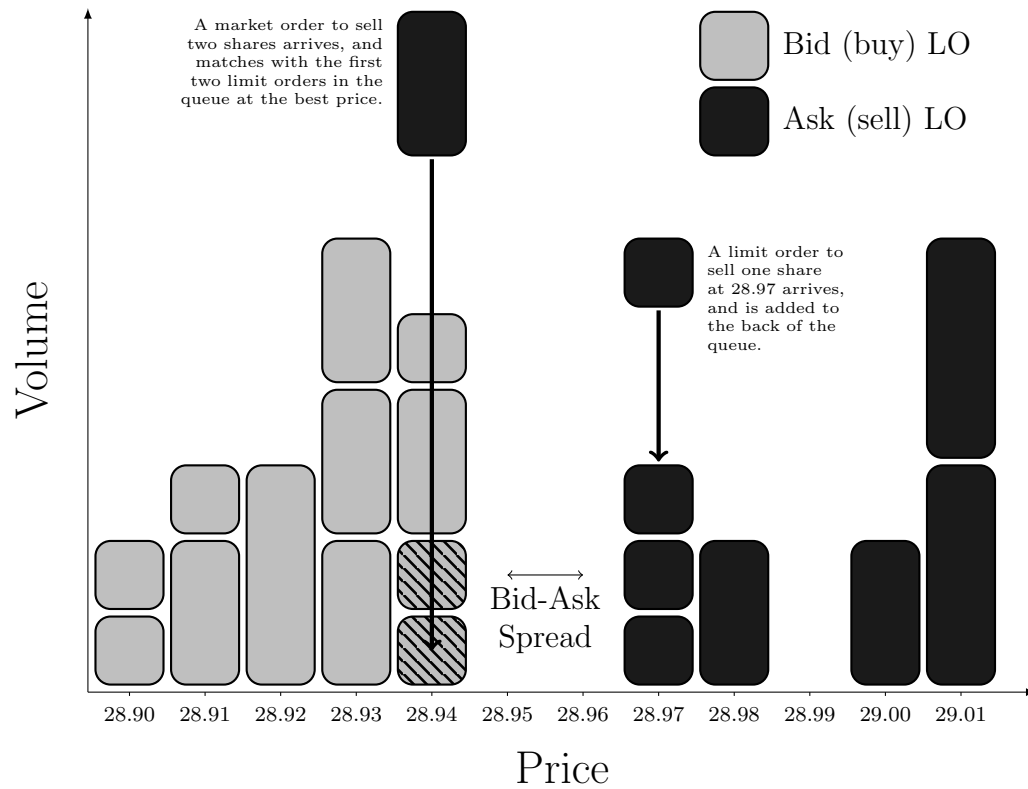
Figure 1.1: Structure and mechanics of the limit order book, adapted from Booth (2015). Each block represents an order, of varying volumes, submitted by various agents participating in the market.

1.2   ITCH Data Set

The underlying data that will be used in this work to generate imbalance and price change timeseries comes from the NASDAQ Historical TotalView-ITCH. ITCH[1] is a direct data-feed protocol that makes it possible for those with a paid subscription to track the status of every order from arrival until cancellation or execution. The Historical TotalView is simply a historical record of the events in the live feed. In the data used in this work, timestamps are provided to 1 millisecond, though newer versions of the feed offer nanosecond precision. Our data has been converted to MATLAB format; below, the structure of the event feed is described in detail (retaining only relevant fields):

Time	Order ID	Event	Volume	Price
⋮	⋮	⋮	⋮	⋮
39960699	72408630	66	100	1107000
39960710	72408630	68	100	1107000
⋮	⋮	⋮	⋮	⋮

Time: Order arrival time in milliseconds from midnight.

Order ID: Unique order reference number.

Event: Event type:

  66 – Add buy order
  83 – Add sell order
  69 – Execute outstanding order in part
  67 – Cancel outstanding order in part
  70 – Execute outstanding order in full
  68 – Delete outstanding order in full
  88 – Bulk volume for the cross event
  84 – Execute non-displayed order

Volume: Number of shares.

Price: Dollar price times 10,000.

Thus, in the above example, we have a buy order arriving at 11:06am for 100 shares at $100.70, and being cancelled 11 milliseconds later. From this feed we are able to

---

[1]Remarkably, according to a representative of the NASDAQ, 'ITCH' does not stand for anything.

reconstruct the entire limit order book at any point in time, which amounts to being able to generate a plot as in Figure 1.1 detailing the exact liquidity available at each order depth.

1.3 Order Imbalance

A core component of this dissertation is limit order book imbalance. *Imbalance* is a ratio of limit order volumes between the bid and ask side, and in the work that follows is calculated as

$$I(t) = \frac{V_{bid}(t) - V_{ask}(t)}{V_{bid}(t) + V_{ask}(t)} \in [-1, 1] \tag{1.1}$$

where both V_{bid} and V_{ask} are computed as the weighted average volumes at the three lowest depths having non-zero volume, using exponentially decreasing weights. As a sample calculation, the imbalance of the sample LOB presented in Figure 1.1 (prior to order arrivals) would be

$$
\begin{aligned}
V_{bid} &= \text{weight}(28.94) \cdot \text{volume}(28.94) \\
&\quad + \text{weight}(28.93) \cdot \text{volume}(28.93) \\
&\quad + \text{weight}(28.92) \cdot \text{volume}(28.92) \\
&= e^{-0.5(0)} \cdot 5 + e^{-0.5(1)} \cdot 6 + e^{-0.5(2)} \cdot 3 \\
&= 1.0000 \cdot 5 + 0.6065 \cdot 6 + 0.3679 \cdot 3 \\
&= 9.7428 \\
V_{ask} &= 4.9488 \\
I(t) &= \frac{9.7428 - 4.9488}{9.7428 + 4.9488} \\
&= 0.3263
\end{aligned}
$$

In the figure we see that there are more limit orders on the bid side than on the ask, and the above value confirms that there is a medium imbalance in favour of the bid side.

1.4 Roadmap

The remainder of this dissertation is structured as follows:

Chapter 2 explores the possibility of constructing naive trading strategies using the statistical properties arising from modelling imbalance as a continuous time Markov chain; a basic understanding of probability theory is required.

Chapter 3 casts the same statistical arbitrage problem into a stochastic optimal control framework, and solves it in both continuous and discrete time; familiarity with stochastic calculus and dynamic programming is assumed.

Chapter 4 presents calibrations of the optimal controls and explores their dynamics. In-sample and out-of-sample backtests are conducted on historical ITCH data, which show a 652% ROI over 2014.

Chapter 5 concludes the dissertation by restating the primary backtesting results in the context of operational costs, and summarizes the key assumptions and simplifications that have been made. The conclusions are intended as considerations for future work on this topic.

Chapter 2

Exploratory Data Analysis

2.1 Modelling Imbalance: Continuous Time Markov Chain

The aim of this research project is to use the LOB volume imbalance $I(t)$ in an algorithmic trading application; hence, a suitable choice of model for $I(t)$ must be made. Rather than modelling imbalance directly as a real-valued process, an alternative approach, and that which is used herein, is to discretize the imbalance value $I(t)$ into subintervals, or bins, and fit the resulting process to a continuous-time Markov chain.

The following definitions and properties are adapted from Takahara (2014):

Definition 1. *A continuous-time stochastic process* $\{X(t) \mid t \geq 0\}$ *with state space S is called a* continuous-time Markov chain (CTMC) *if it has the Markov property; namely, that*

$$\mathbb{P}\left[X(t) = j \mid X(s) = i, X(t_{n-1} = i_{n-1}, \ldots, X(t_1) = i_1\right] = \mathbb{P}\left[X(t) = j \mid X(s) = i\right] \quad (2.1)$$

where for any integer $n \geq 1$, $0 \leq t_1 \leq \cdots \leq t_{n-1} \leq s \leq t$ is any non-decreasing sequence of $n+1$ times, and $i_1, \ldots, i_{n-1}, i, j \in S$ are any $n+1$ states.

Definition 2. *A CTMC $X(t)$ is* time homogeneous *if for any $s \leq t$ and any states $i, j \in S$,*

$$\mathbb{P}\left[X(t) = j \mid X(s) = i\right] = \mathbb{P}\left[X(t-s) = j \mid X(0) = i\right] \quad (2.2)$$

Definition 3. *The key quantities that determine a CTMC $X(t)$ are the* transition rates *q_{ij}, which specify the rate at which X jumps from state i to j. Conditional on leaving state i, X transitions to state j with* conditional transition probability *p_{ij}. The amount of time that X spends in state i, called the* holding time, *is exponentially distributed with rate v_i. These quantities are related by*

$$v_i = \sum_{\substack{j \in S \\ j \neq i}} q_{ij} \tag{2.3}$$

$$q_{ij} = v_i \cdot p_{ij} \tag{2.4}$$

$$p_{ij} = \frac{q_{ij}}{v_i} \tag{2.5}$$

Definition 4. *A CTMC $X(t)$ has an* infinitesimal generator matrix *$\boldsymbol{G}$, whose entries are*

$$g_{ij} = q_{ij}, \qquad i \neq j \tag{2.6}$$

$$g_{ii} = -v_i \tag{2.7}$$

If $X(t)$ has transition probabilities $P_{ij}(t) = \mathbb{P}\left[X(t) = j \mid X(0) = i\right]$ and matrix $\boldsymbol{P}(t) = \{P_{ij}(t)\}$, then $\boldsymbol{P}(t)$ and $\boldsymbol{G}$ are related by

$$\dot{\boldsymbol{P}}(t) = \boldsymbol{G} \cdot \boldsymbol{P}(t) \tag{2.8}$$

$$\boldsymbol{P}(t) = e^{\boldsymbol{G}t} \tag{2.9}$$

Conditional on $X(t) = k$, we assume the arrival of buy and sell market orders follow independent Poisson processes with intensities $\lambda_k^{\pm}$, where λ_k^+ (λ_k^-) is the rate of arrivals of market buys (sells). Such processes are called *Markov-modulated Poisson processes*, as the Poisson intensities are themselves stochastic processes determined by the state of the Markov chain. Thus, a timeline of observations of arrivals of buy/sell market orders and of regime switches might look as in Equation (2.1).

In the sections that follow, I derive maximum likelihood estimations for the parameters of the CTMC, and evaluate the fit of the model to the data.
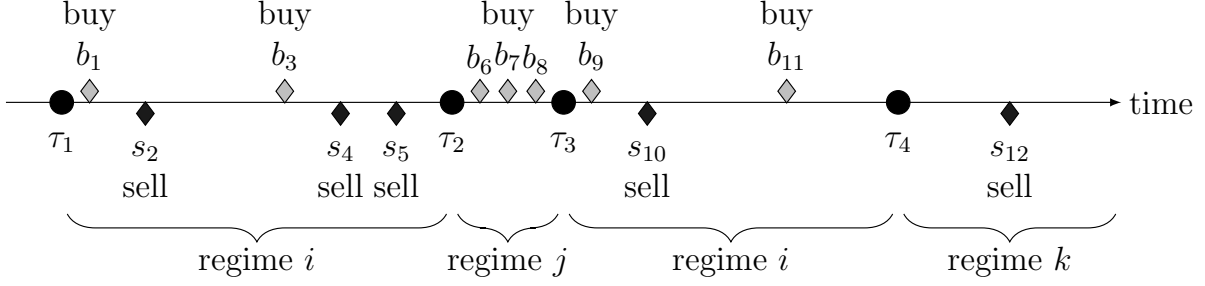
Figure 2.1: Hypothetical timeline of market orders arriving during changing order imbalance regimes.

2.2 Maximum Likelihood Estimate of a Markov-Modulated Poisson Process

2.2.1 MLE of the Infinitesimal Generator Matrix

Let G be the generator matrix for a CTMC $X(t)$ with state space K. From observations, e.g. the fictional events in the timeline given in Figure 2.1, we want to estimate the entries of G. Since the holding time in a given state i has pdf $f(t; v_i) = v_i e^{-v_i t}$, the likelihood function (allowing for repetition of terms) is therefore

$$\mathcal{L}(G) = (v_i e^{-v_i(\tau_2 - \tau_1)} p_{ij})(v_j e^{-v_j(\tau_3 - \tau_2)} p_{ji})(v_i e^{-v_i(\tau_4 - \tau_3)} p_{ik}) \ldots \tag{2.10}$$

$$= \prod_{i=1}^{K} \prod_{i \neq j} (v_i p_{ij})^{N_{ij}(T)} e^{-v_i H_i(T)} \tag{2.11}$$

$$= \prod_{i=1}^{K} \prod_{i \neq j} (q_{ij})^{N_{ij}(T)} e^{-v_i H_i(T)} \tag{2.12}$$

where

$$N_{ij}(T) \equiv \text{number of transitions from regime } i \text{ to } j \text{ up to time } T$$

$$H_i(T) \equiv \text{holding time in regime } i \text{ up to time } T$$

Therefore the log-likelihood becomes

$$\ln \mathcal{L}(G) = \sum_{i=1}^{K} \sum_{i \neq j} [N_{ij}(T) \ln(q_{ij}) - v_i H_i(T)] \tag{2.13}$$

19

$$= \sum_{i=1}^{K} \sum_{i \neq j} \left[N_{ij}(T) \ln(q_{ij}) - \left(\sum_{i \neq k} q_{ik} H_i(T) \right) \right] \tag{2.14}$$

To get a maximum likelihood estimate $\hat{q}_{ij}$ for transition rates and therefore the matrix $\boldsymbol{G}$, we take the partial derivative of $\ln \mathcal{L}(\boldsymbol{G})$ and set it equal to zero:

$$\frac{\partial \ln \mathcal{L}(\boldsymbol{G})}{\partial \hat{q}_{ij}} = \frac{N_{ij}(T)}{q_{ij}} - H_i(T) = 0 \tag{2.15}$$

$$\Rightarrow \hat{q}_{ij} = \frac{N_{ij}(T)}{H_i(T)} \tag{2.16}$$

2.2.2 MLE of the Arrival Rate

Now we want to derive an estimate for the intensity of the Poisson process of market order arrivals conditional on being in state k. We'll look at just the buy market orders for some regime k, as the sell case is identical. Let the buy market order arrival times be indexed by b_i. Since we're assuming that the arrival process is Poisson with the same intensity throughout trials, we can consider the inter-arrival time of events conditional on being in state k. The MLE derivation then follows just as it did for the generator matrix.

$$\mathcal{L}(\lambda_k^+; b_1, \ldots, b_N) = \prod_{i=2}^{N} \lambda_k^+ e^{-\lambda_k^+ (b_i - b_{i-1})} \tag{2.17}$$

$$= (\lambda_k^+)^{N_k^+(T)} e^{-\lambda_k^+ H_k(T)} \tag{2.18}$$

where

$$N_k^+(T) \equiv \text{number of market order arrivals in regime } k \text{ up to time } T$$

$$H_k(T) \equiv \text{holding time in regime } k \text{ up to time } T$$

Therefore the log-likelihood becomes:

$$\ln \mathcal{L}(\lambda_k^+) = N_k^+(T) \ln(\lambda_k^+) - \lambda_k^+ H_k(T) \tag{2.19}$$

$\rho(t)$ is the imbalance bin of the time-weighted average of $I(t)$ over this past interval.

$\Delta S(t)$ is the sign of the mid-price change over this future interval.

$t - \Delta t_I$ t $t + \Delta t_S$ time
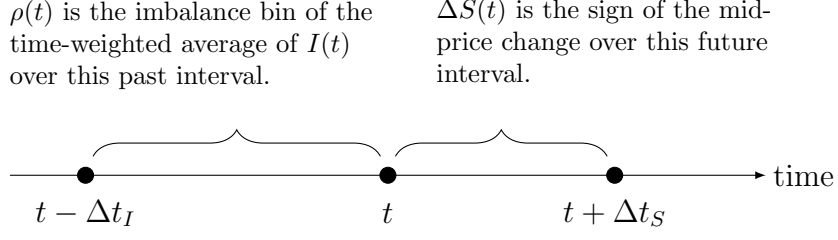
Figure 2.2: Time intervals for time-weighted averaging of imbalance and for price change.

By setting the partial derivative of $\ln \mathcal{L}$ with respect to λ_k^+ equal to zero, we get that the ML estimate for $\hat{\lambda}_k^+$ is:

$$\frac{\partial \ln \mathcal{L}}{\partial \lambda_k^+} = \frac{N_k^+(T)}{\hat{\lambda}_k^+} - H_k(T) = 0 \tag{2.20}$$

$$\Rightarrow \hat{\lambda}_k^+ = \frac{N_k^+(T)}{H_k(T)} \tag{2.21}$$

2.3   2-Dimensional CTMC

Next we consider a CTMC $Z(t)$ that jointly models the imbalance bin $\rho(t)$ and the price change $\Delta S(t)$. The raw imbalance timeseries is very erratic, so to smooth it we taken the time-weighted average of imbalance over the past time inteval Δt_I. We compute price change as the *sign* of the change in midprice of the *future* time interval Δt_S. These time intervals are illustrated in Figure 2.2.

Thus, the CTMC models the joint distribution $(\rho(t), \Delta S(t))$ where

$$\rho(t) \in \{1, 2, \ldots, \#_{bins}\}$$

is the bin corresponding to imbalance averaged over the interval $[t - \Delta t_I, t]$, and

$$\Delta S(t) = \text{sgn}(S(t + \Delta t_S) - S(t)) \in \{-1, 0, 1\}$$

For simplicity of computation, the pair $(\rho(t), \Delta S(t))$ is then reduced into one dimension with a simple encoding function φ; for example, using 3 bins:

$Z(t)$	Bin $\rho(t)$	$\Delta S(t)$	$Z(t)$	Bin $\rho(t)$	$\Delta S(t)$	$Z(t)$	Bin $\rho(t)$	$\Delta S(t)$
1	Bin 1	< 0	4	Bin 1	0	7	Bin 1	> 0
2	Bin 2	< 0	5	Bin 2	0	8	Bin 2	> 0
3	Bin 3	< 0	6	Bin 3	0	9	Bin 3	> 0

Table 2.1: $\varphi(\rho(t), S(t))$: 1-Dimensional Encoding of 2-Dimensional CTMC

2.3.1 Cross-Validation

We cross-validate the CTMC calibration by means of a time-homogeneity test similar to that done in Tan and Ylmaz (2002). The null hypothesis is given by (Weißbach and Walter, 2010)

$$H_0 = \forall i, j \in S \ : \ \exists q_{ij} \in \mathbb{R}^+ \ : \ q_{ij}(t) \equiv q_{ij} \ \forall t \in [0, T] \tag{2.22}$$

whereas the alternative hypothesis states that transition rates/probabilities are time-dependent. To test the hypothesis, we fix $\Delta t_I = \Delta t_S$ at some value, choose a number of imbalance bins, and calculate the MLE estimate of the infinitesimal generator matrix $\boldsymbol{G}$ on the full timeseries. For a chosen error threshold ϵ, we use the relationship in Equation (2.9) to calculate the number of timesteps n_{conv} of size Δt_I such that

$$|| \boldsymbol{P} \left((n_{conv} + 1)\Delta t_I \right) - \boldsymbol{P} \left(n_{conv}\Delta t_I \right) || < \epsilon \tag{2.23}$$

This value n_{conv} determines the size of the cross-validation timewindow into which to partition the full timeseries, yielding K equal subintervals of length n_{conv}. For each "removed series" $k \in \{1, \ldots, K\}$, we recalibrate a CTMC generator matrix $\boldsymbol{G}_k$. Finally, we test whether the one-step transition probabilities p_{ij}^k contained in $\boldsymbol{P}_k \left(\Delta t_I \right)$ are statistically different from those of the full period. For comparison, we also partitioned the timeseries into 8, 4, and 2 equal intervals. The asymptotically equivalent test statistic to the likelihood ratio test statistic is

$$D = -2\ln(\mathcal{L}) = 2 \sum_k \sum_{i,j} n_{i,j}^k \left[\ln(p_{ij}^k) - \ln(p_{ij}) \right] \tag{2.24}$$

where n_{ij}^k is the number of observed transitions from state i to j in subinterval k. This test statistic has a χ^2 distribution with $(K-1)(3 \cdot \#_{bins})(3 \cdot \#_{bins} - 1)$. The tests were run for each ticker for each trading day of 2013, and averaged over the year. Table 2.2 shows the p-value scores for the tests. Considering the standard cutoff p-value of 0.05, the

Δt_I	n_{conv}	K	subintervals 8	4	2	n_{conv}	K	subintervals 8	4	2
			FARO					ORCL		
$\#_{bins} = 3$										
100ms	4933	0.000	0.000	0.000	0.003	1803	0.000	0.000	0.000	0.000
1000ms	727	0.000	0.002	0.001	0.005	303	0.000	0.000	0.000	0.001
10000ms	149	0.000	0.005	0.010	0.017	84	0.000	0.007	0.005	0.010
$\#_{bins} = 5$										
100ms	6450	0.000	0.001	0.002	0.004	2503	0.000	0.000	0.000	0.000
1000ms	941	0.000	0.001	0.003	0.006	404	0.000	0.001	0.002	0.003
10000ms	187	0.000	0.000	0.000	0.005	103	0.000	0.000	0.001	0.009
			NTAP					INTC		
$\#_{bins} = 3$										
100ms	1320	0.000	0.000	0.000	0.000	2545	0.000	0.000	0.000	0.001
1000ms	237	0.000	0.000	0.000	0.000	408	0.000	0.001	0.001	0.002
10000ms	72	0.000	0.006	0.003	0.007	105	0.000	0.004	0.006	0.009
$\#_{bins} = 5$										
100ms	1777	0.000	0.000	0.000	0.000	3498	0.000	0.001	0.001	0.001
1000ms	308	0.000	0.001	0.000	0.001	771	0.000	0.001	0.002	0.002
10000ms	87	0.000	0.000	0.002	0.010	133	0.000	0.000	0.000	0.007

Table 2.2: χ^2-test p-values for testing the time homogeneity hypothesis. Tests were run for each ticker for each trading day of 2013, and averaged over the year. For calculating n_{conv}, the converge error threshold was $\epsilon = 1 \times 10^{-10}$.

cross-validation results show a strong case for the rejection of the homogeneity hypothesis. However, utilizing a non-homogeneous model falls outside of the scope of this research project, and instead suggests possible extensions to this research wherein the trading day is broken down into subintervals to better account for fluctuations and patterns in trading activity - perhaps early morning, mid-day, and final hour of trading.

2.4   Predicting Future Price Changes

It is crucial to note that the value $\Delta S(t)$ contains the price change from time t over the *future* Δt_S seconds - hence in real-time one cannot know the state of the Markov Chain. However, the analytic results do prove enlightening: from the resulting timeseries we estimate a generator matrix $\boldsymbol{G}$, and transform it into a one-step transition probability matrix $\boldsymbol{P} = e^{\boldsymbol{G}\Delta t_I}$. The entries of $\boldsymbol{P}$ are the conditional probabilities

$$\boldsymbol{P}_{ij} = \mathbb{P}\left[\varphi(\rho_{[t-\Delta t_I, t]}, \Delta S_{[t, t+\Delta t_S]}) = j \mid \varphi(\rho_{[t-2\Delta t_I, t-\Delta t_I]}, \Delta S_{[t-\Delta t_I, t]}) = i\right] \tag{2.25}$$

which can be expressed semantically as

$$= \mathbb{P}\left[\varphi(\rho_{curr}, \Delta S_{future}) = j \mid \varphi(\rho_{prev}, \Delta S_{curr}) = i\right] \tag{2.26}$$

Since we can easily decode the 1-dimensional Markov state back into two dimensions, we can think of $\boldsymbol{P}$ as being four-dimensional and re-write its entries as

$$= \mathbb{P}\left[\rho_{curr} = i, \Delta S_{future} = j \mid \rho_{prev} = k, \Delta S_{curr} = m\right] \tag{2.27}$$

$$= \mathbb{P}\left[\rho_{curr} = i, \Delta S_{future} = j \mid B\right] \tag{2.28}$$

where we're using the shorthand $B = (\rho_{prev} = k, \Delta S_{curr} = m)$ to represent the states in the previous timestep. Applying Bayes' Rule,

$$\mathbb{P}\left[\Delta S_{future} = j \mid B, \rho_{curr} = i\right] = \frac{\mathbb{P}\left[\rho_{curr} = i, \Delta S_{future} = j \mid B\right]}{\mathbb{P}\left[\rho_{curr} = i \mid B\right]} \tag{2.29}$$

where the right-hand-side numerator is each individual entry of the one-step probability matrix $\boldsymbol{P}$, and the denominator can be computed from $\boldsymbol{P}$ by

$$\mathbb{P}\left[\rho_{curr} = i \mid B\right] = \sum_j \mathbb{P}\left[\rho_{curr} = i, \Delta S_{future} = j \mid B\right] \tag{2.30}$$

	$\Delta S_{curr} < 0$			$\Delta S_{curr} = 0$			$\Delta S_{curr} > 0$		
	$\rho_{curr} = 1$	2	3	1	2	3	1	2	3
$\Delta S_{future} < 0$									
$\rho_{prev} = 1$	**0.53**	0.15	0.12	0.05	0.10	0.14	0.08	0.13	0.14
$\rho_{prev} = 2$	0.10	**0.58**	0.14	0.07	0.04	0.10	0.13	0.06	0.12
$\rho_{prev} = 3$	0.08	0.12	**0.52**	0.09	0.06	0.03	0.11	0.10	0.05
$\Delta S_{future} = 0$									
$\rho_{prev} = 1$	0.41	0.75	0.78	**0.91**	0.84	0.79	0.42	0.79	0.77
$\rho_{prev} = 2$	0.79	0.36	0.71	0.83	**0.92**	0.82	0.75	0.37	0.78
$\rho_{prev} = 3$	0.79	0.74	0.40	0.81	0.83	**0.91**	0.70	0.76	0.39
$\Delta S_{future} > 0$									
$\rho_{prev} = 1$	0.06	0.10	0.09	0.04	0.06	0.07	**0.50**	0.09	0.09
$\rho_{prev} = 2$	0.10	0.06	0.15	0.10	0.04	0.08	0.12	**0.57**	0.10
$\rho_{prev} = 3$	0.13	0.14	0.08	0.10	0.11	0.05	0.19	0.14	**0.56**

Table 2.3: The $\boldsymbol{Q}$ matrix: probabilities of future price changes, conditioned on current imbalance, current price change, and previous imbalance.

The left-hand-side value in Equation (2.29) is the probability of seeing a given price change over the immediate future time interval conditional on past imbalances and the most recent price change, and therefore allows us to predict future price moves. We'll denote by $\boldsymbol{Q}$ the matrix containing all values given by Equation (2.29).

The $\boldsymbol{Q}$ matrix in Table 2.3 was obtained using data for `MMM` from 2013-05-15, averaging imbalance and price change timewindows $\Delta t_I = \Delta t_S = 1000$ms, and $K = 3$ imbalance bins.

The three middle rows of Table 2.3 contain the majority of values > 0.5, showing that in most cases we are expecting no price change. The only other cases in which the probability of a price change is > 0.5 show evidence of *momentum*; for example, the value in row 1, column 1 can be interpreted as: if $\rho_{prev} = \rho_{curr} = 1$ and previously we saw a downward price change, then we expect to again see a downward price change. The bolded diagonal values in the table lend themselves to the empirical conclusion

$$\mathbb{P}\left[\Delta S_{future} = \Delta S_{curr} \mid \rho_{curr} = \rho_{prev}\right] > 0.5 \tag{2.31}$$

2.5 Naive Trading Strategies

Using the key insight drawn from Equation (2.31), we implemented several naive trading strategies, descriptions of which follow:

Naive Trading Strategy Using the conditional probabilities obtained from $\boldsymbol{Q}$, we will execute a buy (resp. sell) market order if the probability of an upward (resp. downward) price change is > 0.5. Pseudocode for this strategy is given in Algorithm 1.

Algorithm 1 Naive Trading Strategy

1:   $cash = 0$
2:   $asset = 0$
3:   **for** $t = 2 \, : \, \texttt{length}(timeseries)$ **do**
4:      **if** $\mathbb{P}\left[\Delta S_{future} < 0 \mid \rho_{curr}, \rho_{prev}, \Delta S_{curr}\right] > 0.5$ **then**
5:         $cash \mathrel{+}= data.BuyPrice(t)$
6:         $asset \mathrel{-}= 1$
7:      **else if** $\mathbb{P}\left[\Delta S_{future} > 0 \mid \rho_{curr}, \rho_{prev}, \Delta S_{curr}\right] > 0.5$ **then**
8:         $cash \mathrel{-}= data.SellPrice(t)$
9:         $asset \mathrel{+}= 1$
10:     **end if**
11: **end for**
12: **if** $asset > 0$ **then**
13:     $cash \mathrel{+}= asset \times data.BuyPrice(t)$
14: **else if** $asset < 0$ **then**
15:     $cash \mathrel{+}= asset \times data.SellPrice(t)$
16: **end if**

Naive+ Trading Strategy If no change in midprice is expected then we'll post buy and sell limit orders at the touch, front of the queue. We'll track MO arrival between timesteps, assume we always get executed, and immediately repost the limit orders.

Naive++ Trading Strategy As a reformulation of the Naive strategy to use limit orders instead of market orders, if we expect a downward (resp. upward) price change then we'll post an at-the-touch sell (resp. buy) limit order, which may be lifted by an agent who is executing a market order going against the price change momentum.

2.6 Calibration and Backtesting

Backtesting these naive trading strategies required a choice of parameters for the price change observation period Δt_S, the imbalance averaging period Δt_I, and the number of imbalance bins $\#_{bins}$. We used a brute force calibration technique that, for each ticker and each day, traversed the potential parameter space searching for the highest number of timesteps at which Equation (2.31) could be used. We found that $\#_{bins} = 4$ provided the highest expected number of trades for most tickers. However, as we were utilizing percentile bins symmetric around zero, we wanted to have $\#_{bins}$ as an odd number such that all behaviour around zero imbalance was treated equally; thus all backtesting was done with either $\#_{bins} = 3$ or $\#_{bins} = 5$. Additionally, we found empirically that calibration always yielded $\Delta t_S = \Delta t_I$, so this was taken as a given. The backtest for each ticker then consisted of first calibrating the value Δt_I from the first day of data by maximizing the intra-day Sharpe ratio, then using the calibrated parameters to backtest the entire year.

2.7 Conclusions from the Naive Trading Strategies

As seen in Figure 2.3, the Naive strategy on average underperformed the average mid price, while the Naive+ (at-the-touch limit orders when no change was expected) and Naive++ (adding limit orders to adversely select agents that traded against the price change momentum) strategies both on average generated revenue.

Question 1 Why is the Naive strategy producing, on average, normalized losses? On calibration, we see that our intra-day Sharpe ratio is around 0.01 or 0.02 when we choose our optimal parameters, so at the very least on the calibration date the strategy produces positive returns. The remainder of the calendar days are out-of-sample, and the parameters are (likely) not optimal. This suggests non-stationary data, and in particular not every day can be modelled by the same Markov chain. The problem may be exaggerated by the fact that we're calibrating on the first trading day of the calendar year, when we might expect reduced, or at least non-representative, trading activity. Further, we are using midprices to obtain the $\boldsymbol{Q}$ probability matrix while ignoring the bid-ask spread. Thus predicting a "price change" may be insufficient when considering a monetizable opportunity, as we won't be able to profit off a predicted increase followed by a predicted decrease unless the interim mid-price move is greater than the bid-ask spread (assuming
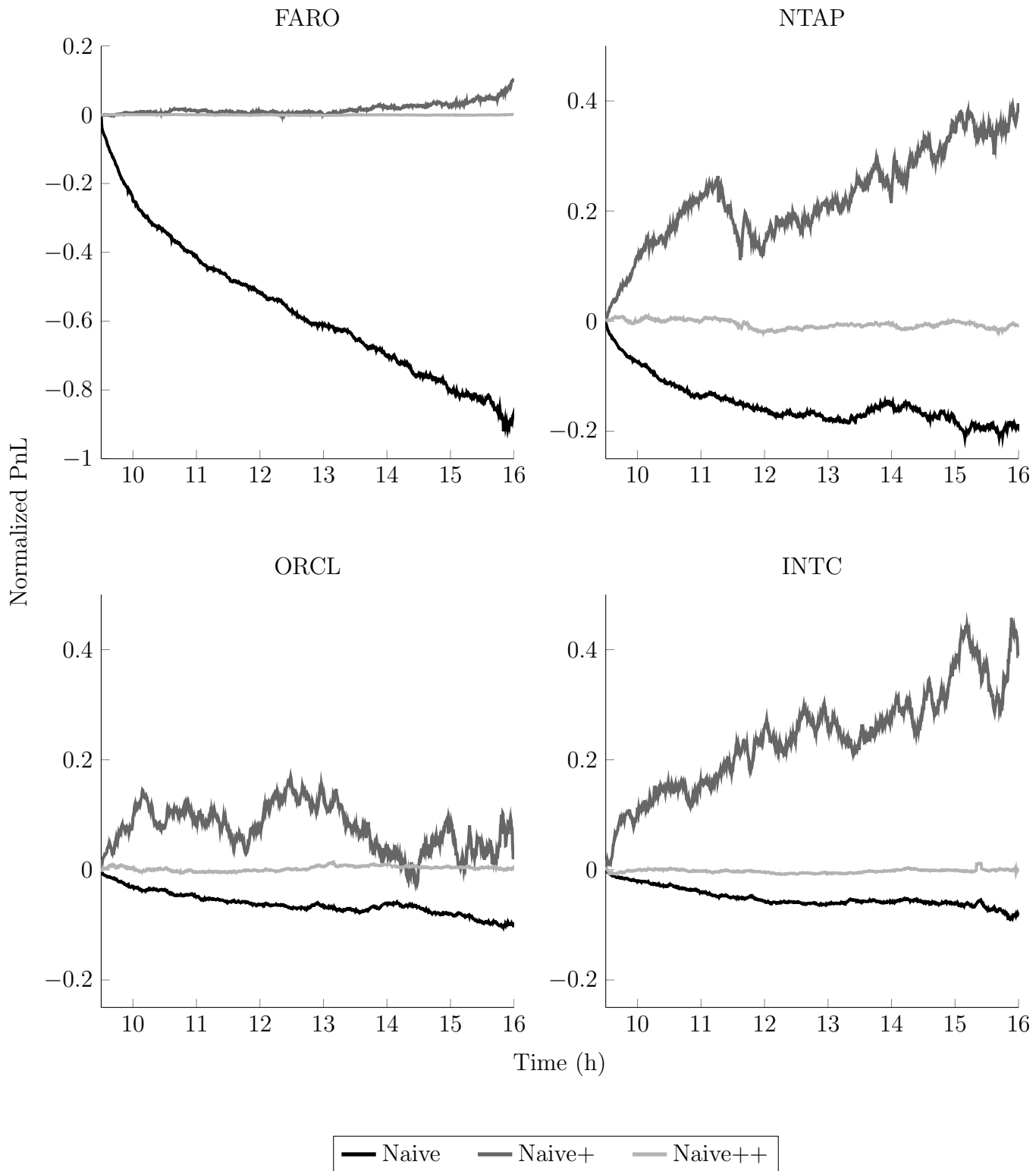
Figure 2.3: Comparison of Naive (black), Naive+ (dark gray), and Naive++ (light gray) trading strategies. Plotted are normalized book values, averaged across the trading year, against the time of the day between market open and close.

t	$I(t)$	Bid/Ask	Prediction	Action	Inv	PnL
0	1	9.99/10.01	$\mathbb{P}[\Delta S_{future} = 0] > 0.5$	None	0	0
1	1	10.00/10.02	$\mathbb{P}[\Delta S_{future} > 0] > 0.5$	BUY @ 10.02	1	-0.02
2	0	10.01/10.03	$\mathbb{P}[\Delta S_{future} = 0] > 0.5$	None	1	-0.01
3	-1	10.01/10.03	$\mathbb{P}[\Delta S_{future} = 0] > 0.5$	None	1	-0.01
4	-1	10.00/10.02	$\mathbb{P}[\Delta S_{future} < 0] > 0.5$	SELL @ 10.00	0	-0.02

Table 2.4: Hypothetical timeline of adverse selection with market orders.

constant spread); this flaw affects trading on `FARO` in particular, which has a spread of about 15 cents.

Question 2 Why do the Naive+ and Naive++ strategies outperform the Naive strategy? This is particularly interesting since the probabilities are being obtained from the same matrix. The obvious difference between the successful and unsuccessful strategies is that the former (a) uses limit orders, and (b) executes when we predict a zero change, whereas the latter uses (a) market orders, and (b) executes when we predict non-zero changes.

(a) leads to a different transaction price being used: a stock purchase with a limit order is executed at the bid price, while a purchase with a market order is at the ask price. Since the asset is marked-to-market at the more conservative price, and the mid price doesn't move as a result of the transaction, then a limit order purchases the share for the same value at which it is marked-to-market, whereas a market order 'crosses the spread' and loses value.

(b) seems to be the largest flaw in the Naive strategy, to which there are two factors. One, we are not predicting the magnitude of the price change, only whether it is zero or non-zero. Two, from the probabilities presented above, *we will only predict a price change if we've already seen a price change.* Thus we're effectively reacting too late. Table 2.4 presents a hypothetical series of events demonstrating the adverse effects of this flaw. Since the strategy is reacting to an already observed price change, the adverse effect would be exacerbated if the initial price change at timestep 4 were larger. All these considerations suggest potential modifications to the strategies.

Chapter 3

Stochastic Optimal Control

Leveraging the insights gained from the exploratory data analysis in the previous chapter, I turn my attention now to casting the statistical arbitrage problem into a mathematical framework. With our underlying process of interest being a Markov chain, the problem lends itself naturally to being considered in the context of stochastic optimal control. Stochastic control problems are common in finance, where many of the underlying processes have a random nature; the goal is to maximize the expectation of some target function, representing profit, by converging on a set of optimal controls that drive the dynamics of the stochastic system to whichever state attains that maximum expectation. [Of course, the problem can conversely be aimed at minimizing expected cost.]

The principal tool in stochastic optimal control is the dynamic programming principle. Under the requisite conditions, the principle allows the optimal controls to be solved from the terminal timestep backward, one step at a time, rather than attempting to simultaneously solve for the controls over the entire time horizon. In most cases, where an analytic solution does not exist, this produces a lookup table for the optimal control conditional on all state variables.

Because a continuous-time Markov chain has a so-called embedded discrete-time Markov chain, we are able to consider the stochastic control problem in both continuous time and discrete time, and an interesting byproduct of the analysis will be in considering how the emerging dynamics differ.

For all the analysis that follows, we fix a filtered probability space $(\Omega, \mathcal{F}, \{\mathcal{F}_t\}_{0 \leq t \leq T}, \mathbb{P})$ satisfying the usual conditions of being complete ($\mathcal{F}_0$ contains all ω such that $\mathbb{P}(\omega) = 0$)

and right-continuous $(\mathcal{F}_t = \mathcal{F}_{t+} := \bigcap_{s>t} \mathcal{F}_s)$.

3.1 Continuous Time

In order to set up the optimization problem we require an aforementioned 'profit' function, and a description of the stochastic system which we are attempting to control. Below, we identify and describe the variables that will be used in the analysis that follows.

Imbalance Averaging Time $\qquad \Delta_{t_I}$
> A constant, specifying the time window over which the imbalance ratio $I(t)$ (Equation (1.1)) will be averaged.

Price Change Time $\qquad \Delta_{t_S}$
> A constant, specifying the time window over which price changes will be computed.

Number of Imbalance Bins $\qquad \#_{bins}$
> A constant, specifying the number of bins (spaced by percentiles, symmetric around zero) into which $I(t)$ will be sorted.

Imbalance $\qquad \rho_t$
> The finite, discrete stochastic process that results from sorting $I(t)$ into the imbalance bins $\{1, \ldots, \#_{bins}\}$, and which evolves in accordance with the CTMC $\boldsymbol{Z}$.

Midprice $\qquad S_t$
> A stochastic process that evolves in accordance with the CTMC $\boldsymbol{Z}$.

Midprice Change $\qquad \Delta S_t = \text{sgn}(S_t - S_{t-\Delta_{t_S}})$

Imbalance & Midprice Change $\qquad \boldsymbol{Z}_t = (\rho_t, \Delta S_t)$
> A continuous-time Markov chain with generator $\boldsymbol{G}$.

Bid-Ask Half-Spread $\qquad \xi$
> A constant, such that 2ξ is equal to the best ask price minus the best bid price.

ΔS when LOB Shuffles $\qquad \{\eta_{0,\boldsymbol{z}}, \eta_{1,\boldsymbol{z}}, \ldots\} \sim F_{\boldsymbol{z}}$
> i.i.d. random variables, where the distribution is dependent on the Markov chain state. These variables represent the sign and magnitude of the midprice change when such a change occurs.

LOB Shuffling $\qquad N_t$

A Poisson process with rate $\lambda(\boldsymbol{Z}_t)$. This process accounts for all events in the LOB that affect midprice, be it from executions, cancellations, or order modifications within the LOB. Together with the previous definition, we thus have that the stock midprice S_t evolves according to the SDE:

$$\mathrm{d}S_t = \eta_{N_{t^-},Z_{t^-}}\,\mathrm{d}N_t \tag{3.1}$$

Additionally, the midprice satisfies:

$$S_t = S_{t_0} + \int\limits_{t_0+s}^{t} \Delta_u\,\mathrm{d}u \tag{3.2}$$

Other Agent Market Orders $\qquad K_t^{\pm}$

Poisson processes with rate $\mu^{\pm}(\boldsymbol{Z}_t)$. K^+ represents the arrival of an other agent's buy market order.

Our Limit Order Posting Depth $\quad \delta_t^{\pm}$

One of the $\mathcal{F}$-predictable processes that we will control. The value of δ^+ dictates how deep on the buy side we will post our buy limit order - if $\delta^+ = 0$ then we are posting at-the-touch.

Our LO fill count $\qquad\qquad\qquad L_t^{\pm}$

counting processes (not Poisson) satisfying the relationship that if at time t we have a sell limit order posted at a depth δ_t^-, then our fill probability is $e^{-\kappa \delta_t^-}$ conditional on a buy market order arriving; namely:

$$\mathbb{P}[\,\mathrm{d}L_t^- = 1 \,|\, \mathrm{d}K_t^+ = 1] = e^{-\kappa \delta_t^-} \tag{3.3}$$

Note that L^-, our sell limit order being filled, depends on K^+, an external buy order arriving.

Our MOs $\qquad\qquad\qquad\qquad M_t^{\pm}$

Our other controlled process. M^+ represents our executing a buy market order. In executing market orders, we assume that the size of the MOs is small enough to achieve the best bid/ask price, and not walk the book.

Our MO execution times $\qquad\quad \boldsymbol{\tau}^{\pm} = \{\tau_k^{\pm} : k = 1, \dots\}$

An increasing sequence of $\mathcal{F}$-stopping times, representing the time at which we execute market orders.

Cash $X_t^{\tau,\delta}$

A stochastic variable representing our cash, initially zero, that evolves according to

$$dX_t^{\tau,\delta} = \underbrace{\left(S_t + \xi_t + \delta_t^-\right) dL_t^-}_{\text{sell limit order}} - \underbrace{\left(S_t - \xi_t - \delta_t^+\right) dL_t^+}_{\text{buy limit order}}$$
$$+ \underbrace{\left(S_t - \xi_t\right) dM_t^-}_{\text{sell market order}} - \underbrace{\left(S_t + \xi_t\right) dM_t^+}_{\text{buy market order}} \qquad (3.4)$$

Inventory $Q_t^{\tau,\delta}$

A stochastic process representing our assets, initially zero, that satisfies

$$Q_0^{\tau,\delta} = 0, \qquad Q_t^{\tau,\delta} = L_t^+ + M_t^+ - L_t^- - M_t^- \qquad (3.5)$$

We define a new variable for our net present value (NPV) at time t, call it $W_t^{\tau,\delta}$, and hence $W_T^{\tau,\delta}$ at terminal time T is our 'terminal wealth'. In algorithmic trading, we want to finish the trading day with zero inventory, and assume that at the terminal time T we will submit a market order (of a possibly large volume) to liquidate remaining stock. Here we do not assume that we can receive the best bid/ask price - instead, the price achieved will be $(S - \text{sgn}(Q)\xi - \alpha Q)$, where $\text{sgn}(Q)\xi$ represents crossing the spread in the direction of trading, and αQ represents receiving a worse price linearly in Q due to walking the book. Hence, $W_t^{\tau,\delta}$ satisfies:

$$W_t^{\tau,\delta} = \underbrace{X_t^{\tau,\delta}}_{\text{cash}} + \underbrace{Q_t^{\tau,\delta}\left(S_t - \text{sgn}(Q_t^{\tau,\delta})\xi_t\right)}_{\text{book value of assets}} - \underbrace{\alpha\left(Q_t^{\tau,\delta}\right)^2}_{\text{liquidation penalty}} \qquad (3.6)$$

The set of admissible trading strategies is the product of the sets $\mathcal{T}$, the set of all $\mathcal{F}$-stopping times, and $\mathcal{A}$, the set of all $\mathcal{F}$-predictable, bounded-from-below depths δ. We only consider $\delta^\pm \geq 0$, since at $\delta = 0$ our fill probability is $e^{-\kappa\delta} = 1$, so we cannot increase the chance of our limit order being filled by posting any lower than at-the-touch; doing so would only diminish our profit.

For deriving an optimal trading strategy via dynamic programming, I will consider the performance criteria that maximizes terminal wealth. With the above notation, the per-

formance criteria function can be written

$$H^{\boldsymbol{\tau},\delta}(t,x,s,\boldsymbol{z},q) = \mathbb{E}\left[W_T^{\boldsymbol{\tau},\delta}\right] \tag{3.7}$$

And the value function, in turn, is given by

$$H(t,x,s,\boldsymbol{z},q) = \sup_{\boldsymbol{\tau}\in\mathcal{T}_{[t,T]}} \sup_{\delta\in\mathcal{A}_{[t,T]}} H^{\boldsymbol{\tau},\delta}(t,x,s,\boldsymbol{z},q) \tag{3.8}$$

3.1.1 Dynamic Programming

The following theorems establish the dynamic programming method we will use to solve this type of problem:

Theorem 5 (Cartea et al. (2015)). ***Dynamic Programming Principle for Optimal Stopping and Control.*** *If an agent's performance criteria for a given admissible control $\boldsymbol{u}$ and admissible stopping time τ are given by*

$$H^{\tau,\boldsymbol{u}}(t,\boldsymbol{x}) = \mathbb{E}_{t,\boldsymbol{x}}[G(X_\tau^{\boldsymbol{u}})]$$

and the value function is

$$H(t,\boldsymbol{x}) = \sup_{\tau\in\mathcal{T}_{[t,T]}} \sup_{\boldsymbol{u}\in\mathcal{A}_{[t,T]}} H^{\tau,\boldsymbol{u}}(t,\boldsymbol{x})$$

then the value function satisfies the Dynamic Programming Principle

$$H(t,\boldsymbol{x}) = \sup_{\tau\in\mathcal{T}_{[t,T]}} \sup_{\boldsymbol{u}\in\mathcal{A}_{[t,T]}} \mathbb{E}_{t,\boldsymbol{x}}\left[G(X_\tau^{\boldsymbol{u}})\mathbb{1}_{\tau<\theta} + H(\theta,X_\theta^{\boldsymbol{u}})\mathbb{1}_{\tau\geq\theta}\right] \tag{3.9}$$

for all $(t,\boldsymbol{x}) \in [0,T] \times \mathbb{R}^m$ and all stopping times $\theta \leq T$.

Theorem 6 (Cartea et al. (2015)). ***Dynamic Programming Equation for Optimal Stopping and Control.*** *Assume that the value function $H(t,\boldsymbol{x})$ is once differentiable in t, all second-order derivatives in $\boldsymbol{x}$ exist, and that $G : \mathbb{R}^m \to \mathbb{R}$ is continuous. Then H solves the quasi-variational inequality*

$$0 = \max\left\{\partial_t H + \sup_{\boldsymbol{u}\in\mathcal{A}_t} \mathcal{L}_t^{\boldsymbol{u}} H \; ; \; G - H\right\} \tag{3.10}$$

34

on $\mathcal{D}$, where $\mathcal{D} = [0, T] \times \mathbb{R}^m$.

3.1.2 Maximizing Terminal Wealth (Continuous)

In this section we solve the DPE that results from using the maximal terminal wealth performance criteria. The quasi-variational inequality in equation 3.10 can be interpreted as follows: the max operator is choosing between posting limit orders or executing market orders; the second term, $G - H$, is the stopping region and represents the value derived from executing a market order; and the first term is the continuation region, representing the value of posting limit orders. We'll use the shorthand $H(\cdot) = H(t, x, s, \boldsymbol{z}, q)$ and solve for $\mathrm{d}H$ inside the continuation region, hence $\mathrm{d}M^{\pm} = 0$, in order to then extract out the infinitesimal generator.

$$\mathrm{d}H(t, x, s, \boldsymbol{z}, q) = \sum_i \partial_{x_i} H \, \mathrm{d}x_i \tag{3.11}$$

$$= \partial_t H \, \mathrm{d}t + \partial_{K^{\pm}} H \, \mathrm{d}K^{\pm} + \partial_{\boldsymbol{Z}} H \, \mathrm{d}\boldsymbol{Z} \tag{3.12}$$

$$\begin{aligned}
= \partial_t H \, \mathrm{d}t &+ e^{-\kappa \delta^-} \left[H(t, x + (s + \xi + \delta^-), s, \boldsymbol{z}, q - 1) - H(\cdot) \right] \mathrm{d}K^+ \\
&+ e^{-\kappa \delta^+} \left[H(t, x - (s - \xi - \delta^+), s, \boldsymbol{z}, q + 1) - H(\cdot) \right] \mathrm{d}K^- \\
&+ \sum_{\mathbf{j}} \mathbb{E} \left[H(t, x, s + \eta_{0,\mathbf{j}}, \mathbf{j}, q) - H(\cdot) \right] \mathrm{d}Z_{\boldsymbol{z},\mathbf{j}}
\end{aligned} \tag{3.13}$$

We substitute in the identities relating each process to its corresponding compensated process, each of which is a continuous-time martingales. For Poisson processes we have (Cartea et al., 2015)

$$\mathrm{d}K^{\pm} = \mathrm{d}\tilde{K}^{\pm} + \mu^{\pm}(\boldsymbol{z}) \, \mathrm{d}t \tag{3.14}$$

while for the Markov Chain, this is (Kurtz, 2004)

$$\mathrm{d}Z_{\boldsymbol{z},\mathbf{j}} = \mathrm{d}\tilde{Z}_{\boldsymbol{z},\mathbf{j}} + G_{\boldsymbol{z},\mathbf{j}} \, \mathrm{d}t \tag{3.15}$$

$$= \partial_t H \, dt + \Bigg\{ \mu^+(\boldsymbol{z}) e^{-\kappa \delta^-} \left[H(t, x + (s + \xi + \delta^-), s, \boldsymbol{z}, q - 1) - H(\cdot) \right]$$

$$+ \mu^-(\boldsymbol{z}) e^{-\kappa \delta^+} \left[H(t, x - (s - \xi - \delta^+), s, \boldsymbol{z}, q + 1) - H(\cdot) \right]$$

$$+ \sum_{\mathbf{j}} G_{\boldsymbol{z},\mathbf{j}} \mathbb{E} \left[H(t, x, s + \eta_{0,\mathbf{j}}, \mathbf{j}, q) - H(\cdot) \right] \Bigg\} \, dt$$

$$+ e^{-\kappa \delta^-} \left[H(t, x + (s + \xi + \delta^-), s, \boldsymbol{z}, q - 1) - H(\cdot) \right] d\tilde{K}^+$$

$$+ e^{-\kappa \delta^+} \left[H(t, x - (s - \xi - \delta^+), s, \boldsymbol{z}, q + 1) - H(\cdot) \right] d\tilde{K}^-$$

$$+ \sum_{\mathbf{j}} \mathbb{E} \left[H(t, x, s + \eta_{0,\mathbf{j}}, \mathbf{j}, q) - H(\cdot) \right] d\tilde{Z}_{\boldsymbol{z},\mathbf{j}}$$

$$\tag{3.16}$$

From which we can see that the infinitesimal generator is given by

$$\mathcal{L}_t^\delta H = \mu^+(\boldsymbol{z}) e^{-\kappa \delta^-} \left[H(t, x + (s + \xi + \delta^-), s, \boldsymbol{z}, q - 1) - H(\cdot) \right]$$
$$+ \mu^-(\boldsymbol{z}) e^{-\kappa \delta^+} \left[H(t, x - (s - \xi - \delta^+), s, \boldsymbol{z}, q + 1) - H(\cdot) \right]$$
$$+ \sum_{\mathbf{j}} G_{\boldsymbol{z},\mathbf{j}} \mathbb{E} \left[H(t, x, s + \eta_{0,\mathbf{j}}, \mathbf{j}, q) - H(\cdot) \right] \tag{3.17}$$

Now, our DPE has the form

$$0 = \max \Bigg\{ \partial_t H + \sup_{\boldsymbol{u} \in \mathcal{A}_t} \mathcal{L}_t^{\boldsymbol{u}} H \; ; \; H(t, x - (s + \xi), s, \boldsymbol{z}, q + 1) - H(\cdot) \; ;$$
$$H(t, x + (s - \xi), s, \boldsymbol{z}, q - 1) - H(\cdot) \Bigg\} \tag{3.18}$$

with boundary conditions

$$H(T, x, s, \boldsymbol{z}, q) = x + q(s - \operatorname{sgn}(q)\xi) - \alpha q^2 \tag{3.19}$$
$$H(t, x, s, \boldsymbol{z}, 0) = x \tag{3.20}$$

The three terms over which we are maximizing represent the continuation regions and stopping regions of the optimization problem. The first term, the continuation region, represents the limit order controls; the second and third terms, each a stopping region, represent the value gain from executing a buy market order and a sell market order, respectively.

Let's introduce the ansatz $H(\cdot) = x + q(s - \operatorname{sgn}(q)\xi) + h(t, \boldsymbol{z}, q)$. The first two terms are the wealth plus book value of assets, hence a mark-to-market of the current position, whereas

the $h(t, \mathbf{z}, q)$ captures value due to the optimal trading strategy. The corresponding boundary conditions on h are

$$h(T, \mathbf{z}, q) = -\alpha q^2 \tag{3.21}$$

$$h(t, \mathbf{z}, 0) = 0 \tag{3.22}$$

Substituting this ansatz into equation 3.17, we get:

$$
\begin{aligned}
\mathcal{L}_t^\delta H = \ & \mu^+(\mathbf{z}) e^{-\kappa \delta^-} \big[\delta^- + \xi[1 + \mathrm{sgn}(q-1) + q(\mathrm{sgn}(q) - \mathrm{sgn}(q-1))] \\
& \qquad + h(t, \mathbf{z}, q-1) - h(t, \mathbf{z}, q) \big] \\
& + \mu^-(\mathbf{z}) e^{-\kappa \delta^+} \big[\delta^+ + \xi[1 - \mathrm{sgn}(q+1) + q(\mathrm{sgn}(q) - \mathrm{sgn}(q+1))] \\
& \qquad + h(t, \mathbf{z}, q+1) - h(t, \mathbf{z}, q) \big] \\
& + \sum_{\mathbf{j}} G_{\mathbf{z},\mathbf{j}} \left[q \mathbb{E}[\eta_{0,\mathbf{j}}] + h(t, \mathbf{j}, q) - h(t, \mathbf{z}, q) \right]
\end{aligned}
\tag{3.23}
$$

We can further simplify the factors of ξ; for example, in the case of the δ^+ term, we can write

$$
\begin{aligned}
1 - \mathrm{sgn}(q+1) + q(\mathrm{sgn}(q) - \mathrm{sgn}(q+1)) &= 1 - (-\mathbb{1}_{q \leq -2} + \mathbb{1}_{q \geq 0}) + \mathbb{1}_{q = -1} \\
&= 1 + (\mathbb{1}_{q \leq -1} - \mathbb{1}_{q \geq 0}) \\
&= 2 \cdot \mathbb{1}_{q \leq -1}
\end{aligned}
$$

This gives us the simplified infinitesimal generator term

$$
\begin{aligned}
\mathcal{L}_t^\delta H = \ & \mu^+(\mathbf{z}) e^{-\kappa \delta^-} \big[\delta^- + 2\xi \cdot \mathbb{1}_{q \geq 1} + h(t, \mathbf{z}, q-1) - h(t, \mathbf{z}, q) \big] \\
& + \mu^-(\mathbf{z}) e^{-\kappa \delta^+} \big[\delta^+ + 2\xi \cdot \mathbb{1}_{q \leq -1} + h(t, \mathbf{z}, q+1) - h(t, \mathbf{z}, q) \big] \\
& + \sum_{\mathbf{j}} G_{\mathbf{z},\mathbf{j}} \left[q \mathbb{E}[\eta_{0,\mathbf{j}}] + h(t, \mathbf{j}, q) - h(t, \mathbf{z}, q) \right]
\end{aligned}
\tag{3.24}
$$

In the DPE, the first term requires finding the supremum over all $\delta^\pm$ of the infinitesimal generator. For this we can set the partial derivatives with respect to both δ^+ and δ^- equal to zero to solve for the optimal posting depth, which we denote with a superscript asterisk. For δ^+ we get:

$$0 = \partial_{\delta^+} \left[e^{-\kappa \delta^{+*}} \left[\delta^{+*} + 2\xi \cdot \mathbb{1}_{q \leq -1} + h(t, \mathbf{z}, q+1) - h(t, \mathbf{z}, q) \right] \right] \tag{3.25}$$

$$= -\kappa e^{-\kappa \delta^{+*}} \left[\delta^{+*} + 2\xi \cdot \mathbb{1}_{q \leq -1} + h(t, \mathbf{z}, q+1) - h(t, \mathbf{z}, q) \right] + e^{-\kappa \delta^{+*}} \tag{3.26}$$

$$= e^{-\kappa \delta^+} \big[-\kappa \big(\delta^{+*} + 2\xi \cdot \mathbb{1}_{q \leq -1} + h(t, \boldsymbol{z}, q+1) - h(t, \boldsymbol{z}, q) \big) + 1 \big] \tag{3.27}$$

Since $e^{-\kappa \delta^{+*}} > 0$, the term inside the square braces must be equal to zero:

$$0 = -\kappa \big(\delta^{+*} + 2\xi \cdot \mathbb{1}_{q \leq -1} + h(t, \boldsymbol{z}, q+1) - h(t, \boldsymbol{z}, q) \big) + 1 \tag{3.28}$$

$$\delta^{+*} = \frac{1}{\kappa} - 2\xi \cdot \mathbb{1}_{q \leq -1} - h(t, \boldsymbol{z}, q+1) + h(t, \boldsymbol{z}, q) \tag{3.29}$$

Recalling that our optimal posting depths are to be non-negative, we thus find that the optimal buy limit order posting depth can be written in feedback form as

$$\delta^{+*} = \max \left\{ 0 \; ; \; \frac{1}{\kappa} - 2\xi \cdot \mathbb{1}_{q \leq -1} - h(t, \boldsymbol{z}, q+1) + h(t, \boldsymbol{z}, q) \right\} \tag{3.30}$$

We can follow similar steps to solve for the optimal sell limit order posting depth

$$\delta^{-*} = \max \left\{ 0 \; ; \; \frac{1}{\kappa} - 2\xi \cdot \mathbb{1}_{q \geq 1} - h(t, \boldsymbol{z}, q-1) + h(t, \boldsymbol{z}, q) \right\} \tag{3.31}$$

Turning our attention to the stopping regions of the DPE, we can use the ansatz to simplify the expressions:

$$\begin{aligned} H(t, x - (s+\xi), s, \boldsymbol{z}, q+1) &- H(\cdot) \\ &= x - s - \xi + (q+1)(s - \operatorname{sgn}(q+1)\xi) + h(t, \boldsymbol{z}, q+1) \\ &\quad - \big[x + q(s - \operatorname{sgn}(q)\xi) + h(t, \boldsymbol{z}, q) \big] \\ &= -\xi \big[(q+1)\operatorname{sgn}(q+1) - q\operatorname{sgn}(q) + 1 \big] + h(t, \boldsymbol{z}, q+1) - h(t, \boldsymbol{z}, q) \\ &= -2\xi \cdot \mathbb{1}_{q \geq 0} + h(t, \boldsymbol{z}, q+1) - h(t, \boldsymbol{z}, q) \end{aligned}$$

$$\tag{3.32}$$
$$\tag{3.33}$$
$$\tag{3.34}$$

and similarly,

$$H(t, x + (s-\xi), s, \boldsymbol{z}, q-1) - H(\cdot) = -2\xi \cdot \mathbb{1}_{q \leq 0} + h(t, \boldsymbol{z}, q-1) - h(t, \boldsymbol{z}, q) \tag{3.35}$$

Substituting all these results and simplifications into the DPE, we find that h satisfies

$$
\begin{aligned}
0 = \max\Bigg\{ & \partial_t h + \mu^+(\boldsymbol{z}) e^{-\kappa \delta^{-*}} \left(\delta^{-*} + 2\xi \mathbb{1}_{q \geq 1} + h(t, \boldsymbol{z}, q-1) - h(t, \boldsymbol{z}, q) \right) \\
& + \mu^-(\boldsymbol{z}) e^{-\kappa \delta^{+*}} \left(\delta^{+*} + 2\xi \cdot \mathbb{1}_{q \leq -1} + h(t, \boldsymbol{z}, q+1) - h(t, \boldsymbol{z}, q) \right) \\
& + \sum_{\mathbf{j}} G_{\boldsymbol{z},\mathbf{j}} \left[q l \mathbb{E}\left[\eta_{0,\mathbf{j}} \right] + h(t, \mathbf{j}, q) - h(t, \boldsymbol{z}, q) \right] \; ; \\
& - 2\xi \cdot \mathbb{1}_{q \geq 0} + h(t, \boldsymbol{z}, q+1) - h(t, \boldsymbol{z}, q) \; ; \\
& - 2\xi \cdot \mathbb{1}_{q \leq 0} + h(t, \boldsymbol{z}, q-1) - h(t, \boldsymbol{z}, q) \Bigg\}
\end{aligned}
\tag{3.36}
$$

Looking at the simplified feedback form in the stopping region, we see that a buy market order will be executed at time τ_q^+ whenever

$$
h(\tau_q^+, \boldsymbol{z}, q+1) - h(\tau_q^+, \boldsymbol{z}, q) = 2\xi \cdot \mathbb{1}_{q \geq 0}
\tag{3.37}
$$

and a sell market order whenever

$$
h(\tau_q^+, \boldsymbol{z}, q-1) - h(\tau_q^+, \boldsymbol{z}, q) = 2\xi \cdot \mathbb{1}_{q \leq 0}
\tag{3.38}
$$

Consider than when our inventory is positive, we can purchase a stock at $s + \xi$, but it will be marked-to-market at $s - \xi$, resulting in a value difference of 2ξ. With negative inventory, we will still purchase at s_ξ, but will now also value at $s + \xi$ because our overall position is still negative, producing no value difference. In particular, with negative inventory, we will execute a buy market order so long as it does not change our value function; and with zero or positive inventory, only if it increases the value function by the value of the spread. The opposite holds for sell market orders. Together, these indicate a penchant for using market orders to drive inventory levels back toward zero when it has no effect on value, and using them to gain extra value only when the expected gain is equal to the size of the spread. This is reminiscent of what we saw in the exploratory data analysis: if a stock is worth S, we can purchase it at $S + \xi$ and immediately be able to sell it at $S - \xi$, at a loss of 2ξ; this was the most significant source of loss in the naive trading market order strategy. Hence we need to expect our value to increase by at least 2ξ when executing market orders for gain.

The variational inequality in Equation (3.36) yields that whilst in the continuation region,

we instead have

$$h(\tau_q^+, \boldsymbol{z}, q+1) - h(\tau_q^+, \boldsymbol{z}, q) \le 2\xi \cdot \mathbb{1}_{q \ge 0} \tag{3.39}$$

$$h(\tau_q^+, \boldsymbol{z}, q-1) - h(\tau_q^+, \boldsymbol{z}, q) \le 2\xi \cdot \mathbb{1}_{q \le 0} \tag{3.40}$$

Taken together, these inequalities yield

$$-2\xi \cdot \mathbb{1}_{q \ge 0} \le h(t, \boldsymbol{z}, q) - h(t, \boldsymbol{z}, q+1) \le 2\xi \cdot \mathbb{1}_{q \le -1} \tag{3.41}$$

$$-2\xi \cdot \mathbb{1}_{q \le 0} \le h(t, \boldsymbol{z}, q) - h(t, \boldsymbol{z}, q-1) \le 2\xi \cdot \mathbb{1}_{q \ge 1} \tag{3.42}$$

or alternatively,

$$\overset{\substack{\text{sell if} =\\\downarrow}}{h(t, \boldsymbol{z}, q)} \le \overset{\substack{\text{buy if} =\\\downarrow}}{h(t, \boldsymbol{z}, q+1)} \le h(t, \boldsymbol{z}, q) + 2\xi, \qquad q \ge 0 \tag{3.43}$$

$$h(t, \boldsymbol{z}, q) \underset{\substack{\uparrow\\\text{buy if} =}}{\le} h(t, \boldsymbol{z}, q-1) \underset{\substack{\uparrow\\\text{sell if} =}}{\le} h(t, \boldsymbol{z}, q) + 2\xi, \qquad q \le 0 \tag{3.44}$$

Recalling the boundary condition $h(t, \boldsymbol{z}, 0) = 0$, Equation (3.43) and Equation (3.44) tell us that the function h is non-negative everywhere. Furthermore, noting the feedback form of our optimal buy limit order depth given in equation Equation (3.30), together with the inequalities in Equation (3.41) and Equation (3.41), we obtain bounds on our posting depths given by

$$\delta^{+*} = \frac{1}{\kappa} - 2\xi \cdot \mathbb{1}_{q \le -1} - h(t, \boldsymbol{z}, q+1) + h(t, \boldsymbol{z}, q) \tag{3.45}$$

$$\ge \frac{1}{\kappa} - 2\xi \cdot \mathbb{1}_{q \le -1} - 2\xi \cdot \mathbb{1}_{q \ge 0} \tag{3.46}$$

$$= \frac{1}{\kappa} - 2\xi \tag{3.47}$$

$$\delta^{+*} \le \frac{1}{\kappa} - 2\xi \cdot \mathbb{1}_{q \le -1} + 2\xi \cdot \mathbb{1}_{q \le -1} \tag{3.48}$$

$$= \frac{1}{\kappa} \tag{3.49}$$

Combined with the identical conditions on the sell depth, we have the conditions

$$\boxed{\frac{1}{\kappa} - 2\xi \le \delta^{\pm*} \le \frac{1}{\kappa}} \tag{3.50}$$

A possible interpretation of the unexpected upper bound on the posting depth is that if

the calculated buy (resp. sell) depth is 'sufficiently' large so as to indicate a disposition against buying (resp. selling), then it is actually optimal to sell (resp. buy) instead.

Combining Equation (3.30) and Equation (3.37), we know that if δ^+ is determined by its feedback form rather than being floored at zero, then a buy market order is executed under the condition:

$$\text{Buy MO} \Leftrightarrow \qquad -2\xi \cdot \mathbb{1}_{q \geq 0} = h(t, \boldsymbol{z}, q) - h(t, \boldsymbol{z}, q+1) \tag{3.51}$$

$$= \delta^{+*} - \frac{1}{\kappa} + 2\xi \cdot \mathbb{1}_{q \leq -1} \tag{3.52}$$

$$\Leftrightarrow \qquad \begin{cases} -2\xi, & q \geq 0 \\ 0, & q < 0 \end{cases} = \begin{cases} \delta^{+*} - \frac{1}{\kappa}, & q \geq 0 \\ \delta^{+*} - \frac{1}{\kappa} + 2\xi, & q < 0 \end{cases} \tag{3.53}$$

$$\Leftrightarrow \qquad \delta^{+*} = \begin{cases} \frac{1}{\kappa} - 2\xi, & q \geq 0 \\ \frac{1}{\kappa} - 2\xi, & q < 0 \end{cases} \tag{3.54}$$

$$\Leftrightarrow \qquad \delta^{+*} = \frac{1}{\kappa} - 2\xi \tag{3.55}$$

An identical derivation holds for sell market orders. In the next chapter on results, this equality will allow us to gauge the market order behaviour by viewing only the limit order posting depths.

To solve for our ansatz h, we can use any finite differences method (Coleman and Jarrow, 1998) to numerically solve the quasi-variational inequality in Equation (3.36). Since we know that at the terminal time we have $h(T, \boldsymbol{z}, q) = -\alpha q^2$, we can work backward in small time increments of ε, and use a forward approximation for the time derivative, given by $\partial_t h(s) = \frac{h(s+\varepsilon) - h(s)}{\varepsilon}$. This will also require bounding the inventory levels at arbitrary 'large enough' levels at which the behaviour of the function is seen to stabilize. Empirically, we found that $|q| \leq 20$ was sufficient.

3.2 Discrete Time

We now consider the same optimization problem but in discrete time, and we will attempt to reuse the same variable definitions and notation where it makes sense; namely, the constants $\Delta_{t_I}, \Delta_{t_S}, \#_{bins}, \xi$ are defined as before. We will be analysing the embedded discrete time Markov chain, which for any time interval of size Δt can be obtained from the CTMC by considering the transition probability matrix obtained by $\boldsymbol{P} = e^{\boldsymbol{G}\Delta t}$. We have derived the below results with the consideration that $\Delta t = \Delta_{t_I} = \Delta_{t_S} = 1000ms$, though this is not strictly necessary. For convenience, we relist in discrete-time form the processes we will consider for this control problem:

Imbalance $\quad\quad\quad\quad\quad\quad\quad\quad\quad\quad \rho_k$

    The finite, discrete stochastic process that results from sorting $I(t)$ into $\{1, \ldots, \#_{bins}\}$, and which evolves in accordance with the Markov chain $\boldsymbol{z}$.

Midprice $\quad\quad\quad\quad\quad\quad\quad\quad\quad\quad S_k$

    A stochastic process that evolves in accordance with the Markov chain $\boldsymbol{z}$.

Midprice Change $\quad\quad\quad\quad\quad\quad\quad \Delta S_k = \text{sgn}(S_k - S_{k-1})$

Imbalance & Midprice Change $\quad\quad \boldsymbol{z}_k = (\rho_k, \Delta S_k)$

    A discrete-time 2-dimensional time-homogenous Markov chain with transition probabilities $\boldsymbol{P}_{ij}$.

ΔS when LOB Shuffles $\quad\quad\quad\quad \{\eta_{0,\boldsymbol{z}}, \eta_{1,\boldsymbol{z}}, \ldots\} \sim F_{\boldsymbol{z}}$

    i.i.d. random variables, where the distribution is dependent on the Markov chain state. This is the price change that accompanies a change in Markov chain state.

Other Agent Market Orders $\quad\quad K_k^{\pm}$

    The sum of the Poisson process with rate $\mu^{\pm}(\boldsymbol{z}_k)$ over the past time interval Δt. This allows us to consider a continuous time process in discrete time by looking at how many arrivals there were since the previous timestep. K^+ represents the arrival of other agents' buy market orders.

Our Limit Order Posting Depth $\quad \delta_k^{\pm}$

    One of the $\mathcal{F}$-predictable processes that we will control. The value of δ^+ dictates how deep on the buy side we will post our buy limit order - if $\delta^+ = 0$ then we are posting at-the-touch.

Our LO fill count $\quad\quad\quad\quad\quad\quad\quad L_k^{\pm}$

A binary random processes (not Poisson) identifying whether our buy (L^+) or sell (L^-) limit orders were filled. This process is considered in greater detail later in this section.

Our MOs $\qquad\qquad\qquad\qquad M_k^\pm$

Our other controlled process. M^+ represents our executing a buy market order. In executing market orders, we assume that the size of the MOs is small enough to achieve the best bid/ask price, and not walk the book.

Cash $\qquad\qquad\qquad\qquad X_k^{\tau,\delta}$

A stochastic variable representing our cash, initially zero.

Inventory $\qquad\qquad\qquad\qquad Q_k^{\tau,\delta}$

A stochastic process representing our assets, initially zero.

As per a typical discrete-time stochastic control problem, we will consider the following state, control, and random vectors:

$$\text{State } \vec{x}_k = \begin{pmatrix} x_k \\ s_k \\ \boldsymbol{z}_k \\ q_k \end{pmatrix} \begin{array}{l} \text{cash} \\ \text{stock price} \\ \text{Markov chain state, as above} \\ \text{inventory} \end{array}$$

$$\text{Control } \vec{u}_k = \begin{pmatrix} \delta_k^+ \\ \delta_k^- \\ M_k^+ \\ M_k^- \end{pmatrix} \begin{array}{l} \text{bid posting depth} \\ \text{ask posting depth} \\ \text{buy MO - binary control} \\ \text{sell MO - binary control} \end{array}$$

$$\text{Random } \vec{w}_k = \begin{pmatrix} K_k^+ \\ K_k^- \\ \omega_k \end{pmatrix} \begin{array}{l} \text{other agent buy MOs - binary} \\ \text{other agent sell MOs - binary} \\ \text{random variable uniformly distributed on [0,1]} \end{array}$$

Following Kwong (2015), we'll write the evolution of the Markov chain as a function of the current state and a uniformly distributed random variable ω:

$$\boldsymbol{z}_{k+1} = T(\boldsymbol{z}_k, \omega_k) = \sum_{i=0}^{|\Gamma|} i \cdot \mathbb{1}_{\left(\sum_{j=0}^{i-1} \boldsymbol{P}_{\boldsymbol{z}_k,j}, \sum_{j=0}^{i} \boldsymbol{P}_{\boldsymbol{z}_k,j} \right]}(\omega_k) \tag{3.56}$$

Here $\mathbb{1}_A(\omega) = \begin{cases} 1 & \text{if } \omega \in A \\ 0 & \text{if } \omega \notin A \end{cases}$, and hence Z_{k+1} is assigned to the value i for which ω_k is in the indicated interval of probabilities.

Our Markovian state evolution function f, given by $\vec{x}_{k+1} = f(\vec{x}_k, \vec{u}_k, \vec{w}_k)$, can be written explicitly as

$$
\begin{pmatrix} x_{k+1} \\ s_{k+1} \\ \boldsymbol{z}_{k+1} \\ q_{k+1} \end{pmatrix} = \begin{pmatrix} x_k \\ s_k + \eta_{k+1, T(\boldsymbol{z}_k, \omega_k)} \\ T(\boldsymbol{z}_k, \omega_k) \\ q_k \end{pmatrix} + \begin{pmatrix} s_k + \xi + \delta_k^- \\ 0 \\ 0 \\ -1 \end{pmatrix} L_k^- + \begin{pmatrix} -(s_k - \xi - \delta_k^+) \\ 0 \\ 0 \\ 1 \end{pmatrix} L_k^+ \quad (3.57)
$$

The cash process at a subsequent timestep is equal to the cash at the previous step, plus the profits and costs of executing market and/or limit orders. At time k, if the agent posts a sell limit order that gets filled "between timesteps" k and $k+1$ (depending on the binary random variable L_k^-, itself depending on the binary random variable K_k^+), the revenue depends on the stock price at k. This is consistent with reality as with backtesting: while we are choosing to model the posting *depth*, in reality a submitted limit order has a specific price specified - thus once the order is submitted at k, the potential cash received is fixed.

Our impulse control at every time step is given by

$$
\begin{pmatrix} x_k \\ s_k \\ \boldsymbol{z}_k \\ q_k \end{pmatrix} = \begin{pmatrix} x_k \\ s_k \\ \boldsymbol{z}_k \\ q_k \end{pmatrix} + \begin{pmatrix} s_k - \xi \\ 0 \\ 0 \\ -1 \end{pmatrix} M_k^- + \begin{pmatrix} -(s_k + \xi) \\ 0 \\ 0 \\ 1 \end{pmatrix} M_k^+ \quad (3.58)
$$

Our market orders assume immediate execution, and are assumed to be sufficiently small in volume so as to not affect order imbalance or the midprice.

3.2.1 Dynamic Programming

The system formulation allows both continuous and impulse control to mimic what was done in the continuous time section, though in discrete time there is no *a priori* distinction between the two Bensoussan (2008). The following theorem shows that in this case a quasi-variational inequality formulation does exist, and that it is equivalent to the standard

dynamic programming formulation. The result is a simplified expression that mirrors the continuous time analysis.

Theorem 7 (Bensoussan (2008)). ***Dynamic Programming with Impulse Control in Discrete Time.*** *Consider a controlled Markov Chain with state space $X = \mathbb{R}^d$, transition probability $\pi(x, v, \mathrm{d}\eta)$, and positive, bounded, uniformly continuous cost function $l(x, v)$.*

Introduce an impulse control w. Define the extended cost function by $l(x, v, w) = l(x + w, v) + c(w)$, the extended transition probability by $\pi(x, v, w, \mathrm{d}\eta) = \pi(x + w, v, \mathrm{d}\eta)$ with the associated operator $\Phi^{v,w} f(x) = \int_{\mathbb{R}^d} f(\eta)\pi(x, v, w, \mathrm{d}\eta) = \Phi^v f(x + w)$.

Consider a decision rule V, W with associated probability $\mathbb{P}^{V,W,x}$ on $\Omega, \mathcal{A}$ for which $y_1 = x$ a.s. Consider the pay-off function

$$J_x(V, W) = \mathbb{E}^{V,W,x}\left[\sum_{n=1}^{\infty} \alpha^{n-1} l(y_n, v_n, w_n)\right] \tag{3.59}$$

and the corresponding Bellman equation

$$u(x) = \inf_{\substack{v \in U \\ w \geq 0}} [l(x + w, v) + c(w) + \alpha \Phi^v u(x + w)] \tag{3.60}$$

Assume:

1. *$\Phi^V \phi_v(x)$ is continuous in v, x if $\phi_v(x) = \phi(x, v)$ is uniformly continuous and bounded in x, v;*

2. *$c(w) = K \mathbb{1}_{w=0} + c_0(w), \quad c_0(0) = 0, \qquad c_0(w) \to \infty$ as $|w| \to \infty$, $c_0(w)$ is sub-linear positive continuous;*

3. *U is compact.*

Then there exists a unique, positive, bounded solution of Equation (3.60) belonging to the space of uniformly continuous and bounded functions. Further, this solution is identical to that of

$$u(x) = \min \left\{ K + \inf_{w \geq 0} [c_0(w) + u(x + w)] \; ; \; \inf_{v \in U} [l(x, v) + \alpha \Phi^v u(x)] \right\} \tag{3.61}$$

3.2.2 Maximizing Terminal Wealth (Discrete)

Following the dynamic programming with impulse control programme, we introduce the value function $V_k^{\delta\pm}$. Here, as in the continuous-time formulation, our objective is to maximize the terminal wealth performance criteria given by

$$V_k^{\delta\pm}(x, s, \boldsymbol{z}, q) = \mathbb{E}\left[W_T^{\delta\pm}\right] = \mathbb{E}_{k,x,s,\boldsymbol{z},q}\left[X_T^{\delta\pm} + Q_T^{\delta\pm}(S_T - \mathrm{sgn}(Q_T^{\delta\pm})\xi) - \alpha(Q_T^{\delta\pm})^2\right] \quad (3.62)$$

where, as before, the notation $\mathbb{E}_{k,x,s,\boldsymbol{z},q}[\,\cdot\,]$ represents the conditional expectation

$$\mathbb{E}[\,\cdot\,\mid X_k = x, S_k = s, \boldsymbol{Z}_k = \boldsymbol{z}, Q_k = q]$$

In this case, our dynamic programming equations (DPEs) are given by

$$V_T(x, s, \boldsymbol{z}, q) = x + q(s - \mathrm{sgn}(q)\xi) - \alpha q^2 \quad (3.63)$$

$$
\begin{aligned}
V_k(x, s, \boldsymbol{z}, q) = \max\Bigg\{ &\sup_{\delta\pm}\big\{\mathbb{E}_{\mathbf{w}}\left[V_{k+1}(f((x, s, \boldsymbol{z}, q), \boldsymbol{u}, \mathbf{w}_k)]\right\} \ ; \\
&V_k(x + s_k - \xi, s_k, \boldsymbol{z}_k, q_k - 1) \ ; \\
&V_k(x - s_k - \xi, s_k, \boldsymbol{z}_k, q_k + 1)\Bigg\}
\end{aligned}
\quad (3.64)
$$

where expectation is with respect to the random vector $\mathbf{w}_k$. Note that in this formulation we do not have per stage costs, as the cost of execution is bundled into the state x. Nevertheless, it is rather immediate that the execution costs could be disentangled from the system state and seen to satisfy the theorem assumptions. Hypothetically we could add the fourth case where $M^+ = M^- = 1$, though a quick substitution shows that it is always strictly 2ξ less in value than the case of only limit orders, where $M^+ = M^- = 0$. This should be evident, as buying and selling with market orders in a single timestep yields a guaranteed loss as the agent is forced to cross the spread.

To simplify the DPEs, we introduce a now familiar ansatz:

$$V_k(x, s, \boldsymbol{z}, q) = x + q(s - \mathrm{sgn}(q)\xi) + h_k(\boldsymbol{z}, q) \quad (3.65)$$

with boundary condition $h_k(\boldsymbol{z}, 0) = 0$ and terminal condition $h_T(\boldsymbol{z}, q) = -\alpha q^2$. Substi-

tuting this ansatz into the Equation (3.64), we obtain

$$
\begin{aligned}
0 = \max\Big\{ &\sup_{\delta^\pm}\big\{\mathbb{E}_{\mathbf{w}}\left[V_{k+1}(f((x,s,\boldsymbol{z},q),\boldsymbol{u},\mathbf{w}_k))\right] - V_k(x,s,\boldsymbol{z},q)\big\} \ ; \\
&V_k(x+s_k-\xi, s_k, \boldsymbol{z}_k, q_k-1) - V_k(x,s,\boldsymbol{z},q) \ ; \\
&V_k(x-s_k-\xi, s_k, \boldsymbol{z}_k, q_k+1) - V_k(x,s,\boldsymbol{z},q)\Big\}
\end{aligned}
\tag{3.66}
$$

$$
\begin{aligned}
0 = \max\Big\{ \sup_{\delta^\pm}\big\{ \mathbb{E}_{\mathbf{w}}\big[&(s+\xi+\delta^-)L_k^- - (s-\xi-\delta^+)L_k^+ \\
&+ (L_k^+ - L_k^-)\big(s + \eta_{0,T(\boldsymbol{z},\omega)} - \operatorname{sgn}(q + L_k^+ - L_k^-)\xi\big) \\
&+ q\left(\eta_{0,T(\boldsymbol{z},\omega)} - \big(\operatorname{sgn}(q+L_k^+-L_k^-) - \operatorname{sgn}(q)\big)\xi\right) \\
&+ h_{k+1}(T(\boldsymbol{z},\omega), q + L_k^+ - L_k^-) - h_k(\boldsymbol{z},q)\big]\big\} \ ; \\
&- 2\xi\cdot\mathbb{1}_{q\geq 0} + h_k(\boldsymbol{z},q+1) \ ; \\
&- 2\xi\cdot\mathbb{1}_{q\leq 0} + h_k(\boldsymbol{z},q-1)\Big\}
\end{aligned}
\tag{3.67}
$$

We'll begin by concentrating on the first term in the quasi-variational inequality. Thus, we want to solve

$$
\begin{aligned}
\sup_{\delta^\pm}\Big\{ \mathbb{E}_{\mathbf{w}}\Big[&(s+\xi+\delta^-)L_k^- - (s-\xi-\delta^+)L_k^+ \\
&+ (L_k^+ - L_k^-)\big(s + \eta_{0,T(\boldsymbol{z},\omega)} - \operatorname{sgn}(q + L_k^+ - L_k^-)\xi\big) \\
&+ q\left(\eta_{0,T(\boldsymbol{z},\omega)} - \big(\operatorname{sgn}(q+L_k^+-L_k^-) - \operatorname{sgn}(q)\big)\xi\right) \\
&+ h_{k+1}(T(\boldsymbol{z},\omega), q + L_k^+ - L_k^-) - h_k(\boldsymbol{z},q)\Big]\Big\}
\end{aligned}
\tag{3.68}
$$

As other agents' market orders as Poisson distributed, we have that

$$
[K_k^+ = 0] = \frac{e^{-\mu^+(\boldsymbol{z})\Delta t}(\mu^+(\boldsymbol{z})\Delta t)^0}{0!} = e^{-\mu^+(\boldsymbol{z})\Delta t}
\tag{3.69}
$$

and so the probability of seeing some positive number of market orders is

$$
\mathbb{P}[K_k^+ > 0] = 1 - e^{-\mu^+(\boldsymbol{z})\Delta t}
\tag{3.70}
$$

Now we make the simplified assumption that the *aggregate* of the orders walks the limit order book to a depth of p_k, and if $p_k > \delta^-$, then our sell limit order is lifted. As in the continuous time section, we will assume that the probability of our order being lifted is

$e^{-\kappa\delta^-}$. Thus we have the following preliminary results:

$$\mathbb{P}[L_k^- = 1 | K_k^+ > 0] = e^{-\kappa\delta^-} \tag{3.71}$$

$$\mathbb{P}[L_k^- = 0 | K_k^+ > 0] = 1 - e^{-\kappa\delta^-} \tag{3.72}$$

$$\mathbb{E}[L_k^-] = \mathbb{P}[L_k^- = 1 | K_k^+ > 0] \cdot \mathbb{P}[K_k^+ > 0] \tag{3.73}$$

$$= (1 - e^{-\mu^+(z)\Delta t})e^{-\kappa\delta^-} \tag{3.74}$$

For ease of notation, we'll write the probability of the $L_k^- = 1$ event as $p(\delta^-)$. This gives us the additional results:

$$\mathbb{P}[L_k^- = 1] = p(\delta^-) = \mathbb{E}[L_k^-] \tag{3.75}$$

$$\mathbb{P}[L_k^- = 0] = 1 - p(\delta^-) \tag{3.76}$$

$$\partial_{\delta^-}\mathbb{P}[L_k^- = 1] = -\kappa p(\delta^-) \tag{3.77}$$

$$\partial_{\delta^-}\mathbb{P}[L_k^- = 0] = \kappa p(\delta^-) \tag{3.78}$$

Let's pre-compute some of the terms that we'll encounter in the supremum, namely the expectations of the random variables. To each we will assign an uppercase Greek letter as shorthand, as will be evident from the analysis.

$$\begin{aligned} \mathbb{E}[\text{sgn}(q + L_k^+ - L_k^-)] &= \mathbb{P}[L_k^- = 1] \cdot \mathbb{P}[L_k^+ = 1] \cdot \text{sgn}(q) \\ &+ \mathbb{P}[L_k^- = 1] \cdot \mathbb{P}[L_k^+ = 0] \cdot \text{sgn}(q - 1) \\ &+ \mathbb{P}[L_k^- = 0] \cdot \mathbb{P}[L_k^+ = 1] \cdot \text{sgn}(q + 1) \\ &+ \mathbb{P}[L_k^- = 0] \cdot \mathbb{P}[L_k^+ = 0] \cdot \text{sgn}(q) \end{aligned} \tag{3.79}$$

$$\begin{aligned} &= p(\delta^-)p(\delta^+)\,\text{sgn}(q) \\ &+ p(\delta^-)(1 - p(\delta^+))\,\text{sgn}(q - 1) \\ &+ (1 - p(\delta^-))p(\delta^+)\,\text{sgn}(q + 1) \\ &+ (1 - p(\delta^-))(1 - p(\delta^+))\,\text{sgn}(q) \end{aligned} \tag{3.80}$$

$$\begin{aligned} &= \text{sgn}(q)\big[1 - p(\delta^+) - p(\delta^-) + 2p(\delta^+)p(\delta^-)\big] \\ &+ \text{sgn}(q - 1)\big[p(\delta^-) - p(\delta^+)p(\delta^-)\big] \\ &+ \text{sgn}(q + 1)\big[p(\delta^+) - p(\delta^+)p(\delta^-)\big] \end{aligned} \tag{3.81}$$

$$= \begin{cases} 1 & q \geq 2 \\ 1 - p(\delta^-)(1 - p(\delta^+)) & q = 1 \\ p(\delta^+) - p(\delta^-) & q = 0 \\ -[1 - p(\delta^+)(1 - p(\delta^-))] & q = -1 \\ -1 & q \leq -2 \end{cases} \quad (3.82)$$

$$= \Phi(q, \delta^+, \delta^-) \quad (3.83)$$

Similarly:

$$\mathbb{E}[L_k^+ \operatorname{sgn}(q + L_k^+ - L_k^-)] = \mathbb{P}[L_k^- = 1] \cdot \mathbb{P}[L_k^+ = 1] \cdot \operatorname{sgn}(q)$$
$$+ \mathbb{P}[L_k^- = 1] \cdot \mathbb{P}[L_k^+ = 0] \cdot 0 \operatorname{sgn}(q - 1)$$
$$+ \mathbb{P}[L_k^- = 0] \cdot \mathbb{P}[L_k^+ = 1] \cdot \operatorname{sgn}(q + 1) \quad (3.84)$$
$$+ \mathbb{P}[L_k^- = 0] \cdot \mathbb{P}[L_k^+ = 0] \cdot 0 \operatorname{sgn}(q)$$

$$= p(\delta^+)\big[p(\delta^-) \operatorname{sgn}(q) + (1 - p(\delta^-) \operatorname{sgn}(q + 1)\big] \quad (3.85)$$

$$= p(\delta^+) \begin{cases} 1 & q \geq 2 \\ 1 & q = 1 \\ (1 - p(\delta^-)) & q = 0 \\ -p(\delta^-) & q = -1 \\ -1 & q \leq -2 \end{cases} \quad (3.86)$$

$$= p(\delta^+)\Psi(q, \delta^-) \quad (3.87)$$

and

$$\mathbb{E}[L_k^- \operatorname{sgn}(q + L_k^+ - L_k^-)] = p(\delta^-)\big[p(\delta^+) \operatorname{sgn}(q) + (1 - p(\delta^+)) \operatorname{sgn}(q - 1)\big] \quad (3.88)$$

$$= p(\delta^-) \begin{cases} 1 & q \geq 2 \\ p(\delta^+) & q = 1 \\ -(1 - p(\delta^+)) & q = 0 \\ -1 & q = -1 \\ -1 & q \leq -2 \end{cases} \quad (3.89)$$

$$= p(\delta^-)\Upsilon(q, \delta^+) \quad (3.90)$$

We'll also require the partial derivatives of these expectations, which we can easily com-

pute. Below we'll use the simplified notation Φ_+ to denote the function closely associated with the partial derivative of Φ with respect to δ^+.

$$\partial_{\delta^-}\mathbb{E}[\text{sgn}(q + L_k^+ - L_k^-)] = \partial_{\delta^-}\Phi(q, \delta^+, \delta^-) = \kappa p(\delta^-) \begin{cases} 0 & q \geq 2 \\ (1 - p(\delta^+)) & q = 1 \\ 1 & q = 0 \\ p(\delta^+) & q = -1 \\ 0 & q \leq -2 \end{cases} \quad (3.91)$$

$$= \kappa p(\delta^-)\Phi_-(q, \delta^+) \quad (3.92)$$

$$\partial_{\delta^+}\mathbb{E}[\text{sgn}(q + L_k^+ - L_k^-)] = \partial_{\delta^+}\Phi(q, \delta^+, \delta^-) = \kappa p(\delta^+) \begin{cases} 0 & q \geq 2 \\ -p(\delta^-) & q = 1 \\ -1 & q = 0 \\ -(1 - p(\delta^-)) & q = -1 \\ 0 & q \leq -2 \end{cases}$$

$$(3.93)$$

$$= \kappa p(\delta^+)\Phi_+(q, \delta^-) \quad (3.94)$$

$$\partial_{\delta^-}\mathbb{E}[L_k^+ \, \text{sgn}(q + L_k^+ - L_k^-)] = \partial_{\delta^-}p(\delta^+)\Psi(q, \delta^-) = \kappa p(\delta^+)p(\delta^-) \begin{cases} 0 & q \geq 2 \\ 0 & q = 1 \\ 1 & q = 0 \\ 1 & q = -1 \\ 0 & q \leq -2 \end{cases} \quad (3.95)$$

$$= \kappa p(\delta^+)p(\delta^-)\Psi_-(q) \quad (3.96)$$

$$\partial_{\delta^+}\mathbb{E}[L_k^+ \, \text{sgn}(q + L_k^+ - L_k^-)] = \partial_{\delta^+}p(\delta^+)\Psi(q, \delta^-) = -\kappa p(\delta^+)\Psi(q, \delta^-) \quad (3.97)$$

$$\partial_{\delta^-}\mathbb{E}[L_k^- \, \text{sgn}(q + L_k^+ - L_k^-)] = \partial_{\delta^-}p(\delta^-)\Upsilon(q, \delta^+) = -\kappa p(\delta^-)\Upsilon(q, \delta^+) \quad (3.98)$$

$$\partial_{\delta^+}\mathbb{E}[L_k^- \, \text{sgn}(q + L_k^+ - L_k^-)] = \partial_{\delta^+}p(\delta^-)\Upsilon(q, \delta^+) = \kappa p(\delta^+)p(\delta^-) \begin{cases} 0 & q \geq 2 \\ -1 & q = 1 \\ -1 & q = 0 \\ 0 & q = -1 \\ 0 & q \leq -2 \end{cases} \quad (3.99)$$

$$= \kappa p(\delta^+)p(\delta^-)\Upsilon_+(q) \quad (3.100)$$

Recalling that we have $\boldsymbol{P}$ the transition matrix for the Markov Chain $\boldsymbol{Z}$, with $\boldsymbol{P}_{\boldsymbol{z},\mathbf{j}} = \mathbb{P}[\boldsymbol{Z}_{k+1} = \mathbf{j}|\boldsymbol{Z}_k = \boldsymbol{z}]$, then we can also write:

$$\mathbb{E}[h_{k+1}(T(\boldsymbol{z},\omega),q + L_k^+ - L_k^-)] = \sum_{\mathbf{j}} \boldsymbol{P}_{\boldsymbol{z},\mathbf{j}}\left[h_{k+1}(\mathbf{j},q)\big[1 - p(\delta^+) - p(\delta^-) + 2p(\delta^+)p(\delta^-)\big]\right.$$
$$+ h_{k+1}(\mathbf{j},q-1)\big[p(\delta^-) - p(\delta^+)p(\delta^-)\big]$$
$$\left.+ h_{k+1}(\mathbf{j},q+1)\big[p(\delta^+) - p(\delta^+)p(\delta^-)\big]\right]$$

$$(3.101)$$

and its partial derivatives as

$$\partial_{\delta^-}\mathbb{E}[h_{k+1}(T(\boldsymbol{z},\omega),q + L_k^+ - L_k^-)] = \sum_{\mathbf{j}} \boldsymbol{P}_{\boldsymbol{z},\mathbf{j}}\left[h_{k+1}(\mathbf{j},q)\big[\kappa p(\delta^-) - 2\kappa p(\delta^+)p(\delta^-)\big]\right.$$
$$+ h_{k+1}(\mathbf{j},q-1)\big[-\kappa p(\delta^-) + \kappa p(\delta^+)p(\delta^-)\big]$$
$$\left.+ h_{k+1}(\mathbf{j},q+1)\big[\kappa p(\delta^+)p(\delta^-)\big]\right]$$

$$(3.102)$$

$$= \kappa p(\delta^-)\sum_{\mathbf{j}} \boldsymbol{P}_{\boldsymbol{z},\mathbf{j}}\left[h_{k+1}(\mathbf{j},q)\big[1 - 2p(\delta^+)\big]\right.$$
$$+ h_{k+1}(\mathbf{j},q-1)\big[-1 + p(\delta^+)\big]$$
$$\left.+ h_{k+1}(\mathbf{j},q+1)\big[p(\delta^+)\big]\right]$$

$$(3.103)$$

$$\partial_{\delta^+}\mathbb{E}[h_{k+1}(T(\boldsymbol{z},\omega),q + L_k^+ - L_k^-)] = \kappa p(\delta^+)\sum_{\mathbf{j}} \boldsymbol{P}_{\boldsymbol{z},\mathbf{j}}\left[h_{k+1}(\mathbf{j},q)\big[1 - 2p(\delta^-)\big]\right.$$
$$+ h_{k+1}(\mathbf{j},q-1)\big[p(\delta^-)\big]$$
$$\left.+ h_{k+1}(\mathbf{j},q+1)\big[-1 + p(\delta^-)\big]\right]$$

$$(3.104)$$

Now we tackle solving the supremum in equation 3.68 and thus finding the optimal posting depths, again denoted by a subscript asterisk. First we consider the first-order condition

on δ^-, namely that the partial derivative with respect to it must be equal to zero.

$$
\begin{aligned}
0 = \partial_{\delta^-} \Bigg\{ & (s + \xi + \delta^{-*})\mathbb{E}[L_k^-] - (s - \xi - \delta^+)\mathbb{E}[L_k^+] \\
& + \mathbb{E}[L_k^+]\left(s + \mathbb{E}[\eta_{0,T(\mathbf{z},\omega)}]\right) - \xi\mathbb{E}\left[L_k^+ \operatorname{sgn}(q + L_k^+ - L_k^-)\right] \\
& - \mathbb{E}[L_k^-]\left(s + \mathbb{E}[\eta_{0,T(\mathbf{z},\omega)}]\right) + \xi\mathbb{E}\left[L_k^- \operatorname{sgn}(q + L_k^+ - L_k^-)\right] \\
& + q\mathbb{E}[\eta_{0,T(\mathbf{z},\omega)}] - q\xi\mathbb{E}[\operatorname{sgn}(q + L_k^+ - L_k^-)] + q\xi\operatorname{sgn}(q) \\
& + \mathbb{E}\left[h_{k+1}(T(\mathbf{z},\omega), q + L_k^+ - L_k^-)\right] - h_k(\mathbf{z},q) \Bigg\}
\end{aligned}
\tag{3.105}
$$

$$
\begin{aligned}
= \partial_{\delta^-} \Bigg\{ & (s + \xi + \delta^{-*})\mathbb{E}[L_k^-] - \xi\mathbb{E}\left[L_k^+ \operatorname{sgn}(q + L_k^+ - L_k^-)\right] \\
& - \mathbb{E}[L_k^-]\left(s + \mathbb{E}[\eta_{0,T(\mathbf{z},\omega)}]\right) + \xi\mathbb{E}\left[L_k^- \operatorname{sgn}(q + L_k^+ - L_k^-)\right] \\
& - q\xi\mathbb{E}[\operatorname{sgn}(q + L_k^+ - L_k^-)] + \mathbb{E}\left[h_{k+1}(T(\mathbf{z},\omega), q + L_k^+ - L_k^-)\right] \Bigg\}
\end{aligned}
\tag{3.106}
$$

$$
\begin{aligned}
= \ & p(\delta^{-*}) - \kappa p(\delta^{-*})(s + \xi + \delta^{-*}) - \xi\kappa p(\delta^+)p(\delta^{-*})\Psi_-(q) \\
& + \kappa p(\delta^{-*})\left(s + \mathbb{E}[\eta_{0,T(\mathbf{z},\omega)}]\right) - \xi\kappa p(\delta^{-*})\Upsilon(q,\delta^+) - q\xi\kappa p(\delta^{-*})\Phi_-(q,\delta^+) \\
& + \kappa p(\delta^{-*})\sum_{\mathbf{j}} \mathbf{P}_{\mathbf{z,j}}\Bigg[h_{k+1}(\mathbf{j},q)\left[1 - 2p(\delta^+)\right] + h_{k+1}(\mathbf{j},q-1)\left[-1 + p(\delta^+)\right] \\
& \hspace{4cm} + h_{k+1}(\mathbf{j},q+1)\left[p(\delta^+)\right] \Bigg]
\end{aligned}
\tag{3.107}
$$

Dividing through by $\kappa p(\delta^{-*})$, which is nonzero, and re-arranging, we find that the optimal sell posting depth is given by

$$
\begin{aligned}
\delta^{-*} = \ & \frac{1}{\kappa} + \mathbb{E}[\eta_{0,T(\mathbf{z},\omega)}] - \xi\left(1 + p(\delta^+)\Psi_-(q) + \Upsilon(q,\delta^+) + q\Phi_-(q,\delta^+)\right) \\
& + \sum_{\mathbf{j}} \mathbf{P}_{\mathbf{z,j}}\Bigg[h_{k+1}(\mathbf{j},q)\left[1 - 2p(\delta^+)\right] + h_{k+1}(\mathbf{j},q-1)\left[-1 + p(\delta^+)\right] + h_{k+1}(\mathbf{j},q+1)\left[p(\delta^+)\right] \Bigg]
\end{aligned}
\tag{3.108}
$$

$$
\begin{aligned}
= \ & \frac{1}{\kappa} + \mathbb{E}[\eta_{0,T(\mathbf{z},\omega)}] - 2\xi\left(\mathbb{1}_{q \geq 1} + p(\delta^+)\mathbb{1}_{q=0}\right) \\
& + \sum_{\mathbf{j}} \mathbf{P}_{\mathbf{z,j}}\Bigg[h_{k+1}(\mathbf{j},q)\left[1 - 2p(\delta^+)\right] + h_{k+1}(\mathbf{j},q-1)\left[-1 + p(\delta^+)\right] + h_{k+1}(\mathbf{j},q+1)\left[p(\delta^+)\right] \Bigg]
\end{aligned}
\tag{3.109}
$$

Recalling that we want $\delta^{\pm} \geq 0$, we find:

$$\delta^{-*} = \max\left\{ 0 \; ; \; \frac{1}{\kappa} + \mathbb{E}[\eta_{0,T(\boldsymbol{z},\omega)}] - 2\xi\mathbb{1}_{q\geq 1} + \sum_{\mathbf{j}} \boldsymbol{P}_{\boldsymbol{z},\mathbf{j}}\big[h_{k+1}(\mathbf{j},q) - h_{k+1}(\mathbf{j},q-1)\big] \right.$$

$$\left. - p(\delta^+)\left(2\xi\mathbb{1}_{q=0} - \sum_{\mathbf{j}} \boldsymbol{P}_{\boldsymbol{z},\mathbf{j}}\big[h_{k+1}(\mathbf{j},q-1) + h_{k+1}(\mathbf{j},q+1) - 2h_{k+1}(\mathbf{j},q)\big] \right) \right\}$$

(3.110)

And similarly, the optimal buy posting depth is given by:

$$\delta^{+*} = \max\left\{ 0 \; ; \; \frac{1}{\kappa} - \mathbb{E}[\eta_{0,T(\boldsymbol{z},\omega)}] - 2\xi\mathbb{1}_{q\leq -1} + \sum_{\mathbf{j}} \boldsymbol{P}_{\boldsymbol{z},\mathbf{j}}\big[h_{k+1}(\mathbf{j},q) - h_{k+1}(\mathbf{j},q+1)\big] \right.$$

$$\left. - p(\delta^-)\left(2\xi\mathbb{1}_{q=0} - \sum_{\mathbf{j}} \boldsymbol{P}_{\boldsymbol{z},\mathbf{j}}\big[h_{k+1}(\mathbf{j},q-1) + h_{k+1}(\mathbf{j},q+1) - 2h_{k+1}(\mathbf{j},q)\big] \right) \right\}$$

(3.111)

For ease of notation we'll write $\aleph(q) = \sum_{\mathbf{j}} \boldsymbol{P}_{\boldsymbol{z},\mathbf{j}}\left[h_{k+1}(\mathbf{j},q-1) + h_{k+1}(\mathbf{j},q+1) - 2h_{k+1}(\mathbf{j},q)\right]$. Now, assuming we behave optimally on both the buy and sell sides simultaneously, we can substitute equation 3.111 into equation 3.110, while evaluating both at δ^{+*} and δ^{-*} to obtain the optimal posting depth in feedback form:

$$\delta^{-*} = \frac{1}{\kappa} + \mathbb{E}[\eta_{0,T(\boldsymbol{z},\omega)}] - 2\xi\mathbb{1}_{q\geq 1} + \sum_{\mathbf{j}} \boldsymbol{P}_{\boldsymbol{z},\mathbf{j}}\left[h_{k+1}(\mathbf{j},q) - h_{k+1}(\mathbf{j},q-1)\right]$$

$$- \left(1 - e^{\mu^-(\boldsymbol{z})\Delta t}\right)e^{-\kappa\max\left\{0 \; ; \; \frac{1}{\kappa}-\mathbb{E}[\eta_{0,T(\boldsymbol{z},\omega)}]-2\xi\mathbb{1}_{q\leq -1}+\sum_{\mathbf{j}}\boldsymbol{P}_{\boldsymbol{z},\mathbf{j}}\left[h_{k+1}(\mathbf{j},q)-h_{k+1}(\mathbf{j},q+1)\right]\right.} \quad (3.112)$$

$$ {}^{-(1-e^{\mu^+(\boldsymbol{z})\Delta t})e^{-\kappa\delta^{-*}}(2\xi\mathbb{1}_{q=0}-\aleph(q))}\Big\} \left(2\xi\mathbb{1}_{q=0} - \aleph(q)\right)$$

This equation will need to be solved numerically due to the difficulty in isolating δ^{-*} on one side of the equality. Once a solution has been obtained, the value can be substituted back into Equation (3.111) to solve for δ^{+*}.

3.2.3   Simplifying the DPE

We now turn to simplifying the DPE in Equation (3.67) by substituting in the optimal posting depths as written in recursive form: Equation (3.111) and Equation (3.110). In doing so we see a incredible amount of cancellation and simplification, and we obtain the

rather elegant, and surprisingly simple form of the DPE:

$$
\begin{aligned}
h_k(\boldsymbol{z}, q) = \max\Big\{ & q\mathbb{E}[\eta_{0,T(\boldsymbol{z},\omega)}] + \frac{1}{\kappa}(p(\delta^{+^*}) + p(\delta^{-^*})) + \sum_{\mathbf{j}} \boldsymbol{P}_{\boldsymbol{z},\mathbf{j}} h_{k+1}(\mathbf{j}, q) \\
& + p(\delta^{+^*})p(\delta^{-^*}) \sum_{\mathbf{j}} \boldsymbol{P}_{\boldsymbol{z},\mathbf{j}} \left[h_{k+1}(\mathbf{j}, q-1) + h_{k+1}(\mathbf{j}, q+1) - 2h_{k+1}(\mathbf{j}, q) \right] ; \\
& - 2\xi \cdot \mathbb{1}_{q \geq 0} + h_k(\boldsymbol{z}, q+1) ; \\
& - 2\xi \cdot \mathbb{1}_{q \leq 0} + h_k(\boldsymbol{z}, q-1) \Big\}
\end{aligned}
$$

(3.113)

As was the case in continuous time, Equation (3.113) yields that whilst in the continuation region, we have

$$
h_k(\boldsymbol{z}, q) \leq h_k(\boldsymbol{z}, q+1) - 2\xi \cdot \mathbb{1}_{q \geq 0} \tag{3.114}
$$

$$
h_k(\boldsymbol{z}, q) \leq h_k(\boldsymbol{z}, q-1) - 2\xi \cdot \mathbb{1}_{q \leq 0} \tag{3.115}
$$

And these inequalities again give us

$$
-2\xi \cdot \mathbb{1}_{q \geq 0} \leq h_k(\boldsymbol{z}, q) - h_k(\boldsymbol{z}, q+1) \leq 2\xi \cdot \mathbb{1}_{q \leq -1} \tag{3.116}
$$

$$
-2\xi \cdot \mathbb{1}_{q \leq 0} \leq h_k(\boldsymbol{z}, q) - h_k(\boldsymbol{z}, q-1) \leq 2\xi \cdot \mathbb{1}_{q \geq 1} \tag{3.117}
$$

$$
\overset{\substack{\text{sell if} =\\ \downarrow}}{h_k(\boldsymbol{z}, q)} \leq h_k(\boldsymbol{z}, q+1) \overset{\substack{\text{buy if} =\\ \downarrow}}{\leq} h_k(\boldsymbol{z}, q) + 2\xi, \qquad q \geq 0 \tag{3.118}
$$

$$
\underset{\substack{\uparrow\\ \text{buy if} =}}{h_k(\boldsymbol{z}, q)} \leq \underset{\substack{\uparrow\\ \text{sell if} =}}{h_k(\boldsymbol{z}, q-1)} \leq h_k(\boldsymbol{z}, q) + 2\xi, \qquad q \leq 0 \tag{3.119}
$$

Recalling the boundary condition $h_k(\boldsymbol{z}, 0) = 0$, Equation (3.118) and Equation (3.119) tell us that the function h is non-negative everywhere.

At terminal time T, we liquidate our position at a cost of $(s - xi\,\mathrm{sgn}(q) - \alpha q)$ per share, whereas at $T - 1$, we can liquidate at the regular cost of $(s - \xi\,\mathrm{sgn}(q))$. It is thus never optimal to wait until maturity to liquidate the position, and instead we force liquidation one step earlier by setting $h(T - 1, \boldsymbol{z}, q) = 0\ \forall q$. This allows us to effectively ignore the terminal condition, and avoids a contradiction with the finding that $h \geq 0$.

We now have an explicit means of numerically solving for the optimal posting depths. Since we know the function h at the terminal timesteps T and $T - 1$, we can take one

step back to $T-2$ and solve for both the optimal posting depths. With these values we are then able to calculate the value function h_{T-2} using Equation (3.113), and in doing so determine whether to execute market orders in addition to posting limit orders. This process then repeats for each step backward.

Chapter 4

Results

In this chapter we explore the dynamics of the continuous time and discrete time models, and perform in-sample and out-of-sample backtests to compare the performance of the continuous and discrete time solutions to the stochastic optimal control problem.

4.1 Calibration

All tests in this chapter were run using the following global set of parameters:

time window for computing price change	Δt_S	1000ms
time window for averaging order imbalance	Δt_I	1000ms
number of imbalance bins	$\#_{bins}$	5
fill probability constant	κ	100

For each daily calibration, we then computed the remaining parameters using the following formulae:

infinitesimal generator matrix	$\boldsymbol{G}$	Equation 2.16
transition probability matrix	$\boldsymbol{P}$	Equation 2.9
market order arrival intensities	$\mu^{\pm}$	Equation 2.21

Additionally, ξ was computed as half of the simple average of the bid-ask spread observed during the trading day, rounded to the nearest half-cent; and the imbalance bins ρ were computed as the partitioning of the interval $[-1, 1]$ into percentile bins symmetric around zero, where the percentile interval was $100 \div \#_{bins}$.

As was mentioned in Chapter 2, the exploratory data analysis done on the data made use of an unorthodox Markov chain, where its state at time t was actually not determinable at time t because the price change $\Delta S(t)$ was computed over the *future* time interval Δt_S. (See Section 2.3.) In the optimal stochastic control formulations, the Markov chain was defined instead such the price change was computed over the *past* interval Δt_S. However, it was of interest to explore what results would be obtained if the calibration was still done using the non $\mathcal{F}$-predictable method. A justification for doing so is that in a given Markov state Z, there is a state-dependent arrival rate of price updates, and there is a state-dependent distribution of jumps when a price update occurs. So that although the price change is measured over the future when calibrating, this really is a way of getting at the state-dependence of those price changes. In the following tests, this calibration method is denoted 'w nFPC', standing for 'with non-$\mathcal{F}$-predictable calibration'.

4.2   Dynamics of the Optimal Posting Depths

We have solved the same stochastic control problem using both continuous and discrete time, which have yielded markedly different resulting formulae for the optimal limit order posting depths. In this section we explore the calibrated results obtained on an in-sample backtest on `INTC`, calibrating on amalgamated data for the entire 2013 trading year. The dynamics of $\delta^{\pm}$ were obtained using a time-to-maturity of 600sec to best depict the behavior as we approached the end of day trading; as the time-to-maturity horizon increases, the postings depths tend to stabilize.

The first notable conclusion we can make is the symmetry that has emerged between δ^+ and δ^- in 'opposite' Markov states. This is evident when comparing δ^+ in $Z = (-1, -1)$ (Figure 4.1) with δ^- in $Z = (+1, +1)$ (Figure 4.6), δ^+ in $Z = (0, 0)$ (Figure 4.2) with δ^- in $Z = (0, 0)$ (Figure 4.5), and δ^+ in $Z = (+1, +1)$ (Figure 4.3) with δ^- in $Z = (-1, -1)$ (Figure 4.4). Thus, we focus the discussion here on the behavior of δ^+.

In this calibration we have taken $\kappa = 100$ and $\xi = 0.005$. From Equation (3.55), we thus know that a necessary condition for a buy market order to be executed is $\delta^{+*} = \frac{1}{\kappa} - 2\xi = 0$.
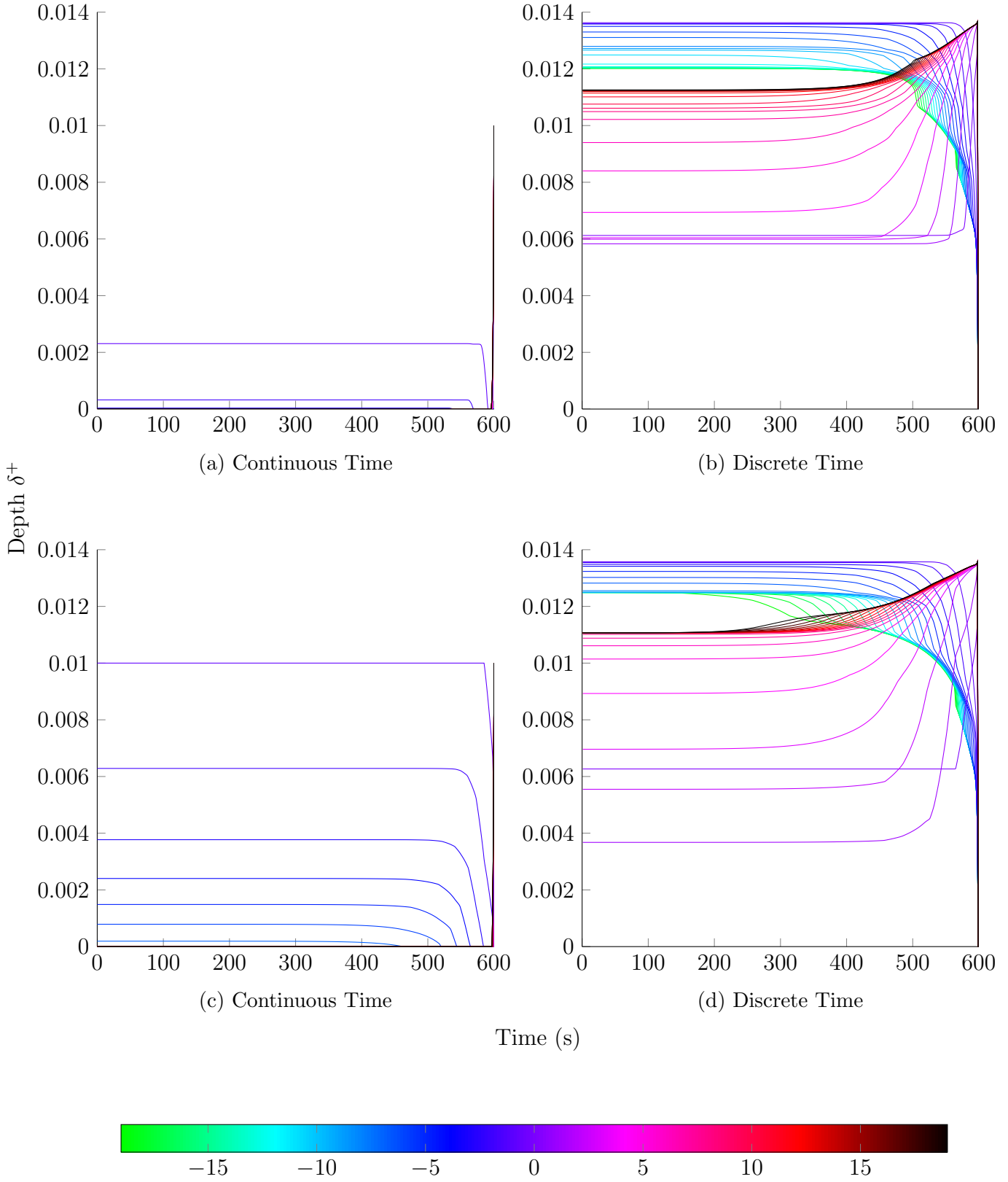
(a) Continuous Time

(b) Discrete Time

(c) Continuous Time

(d) Discrete Time

Time (s)

Figure 4.1: Optimal buy depths δ^+ for Markov state $Z = (\rho = -1, \Delta S = -1)$, implying heavy imbalance in favor of sell pressure, and having previously seen a downward price change. We expect the midprice to fall.
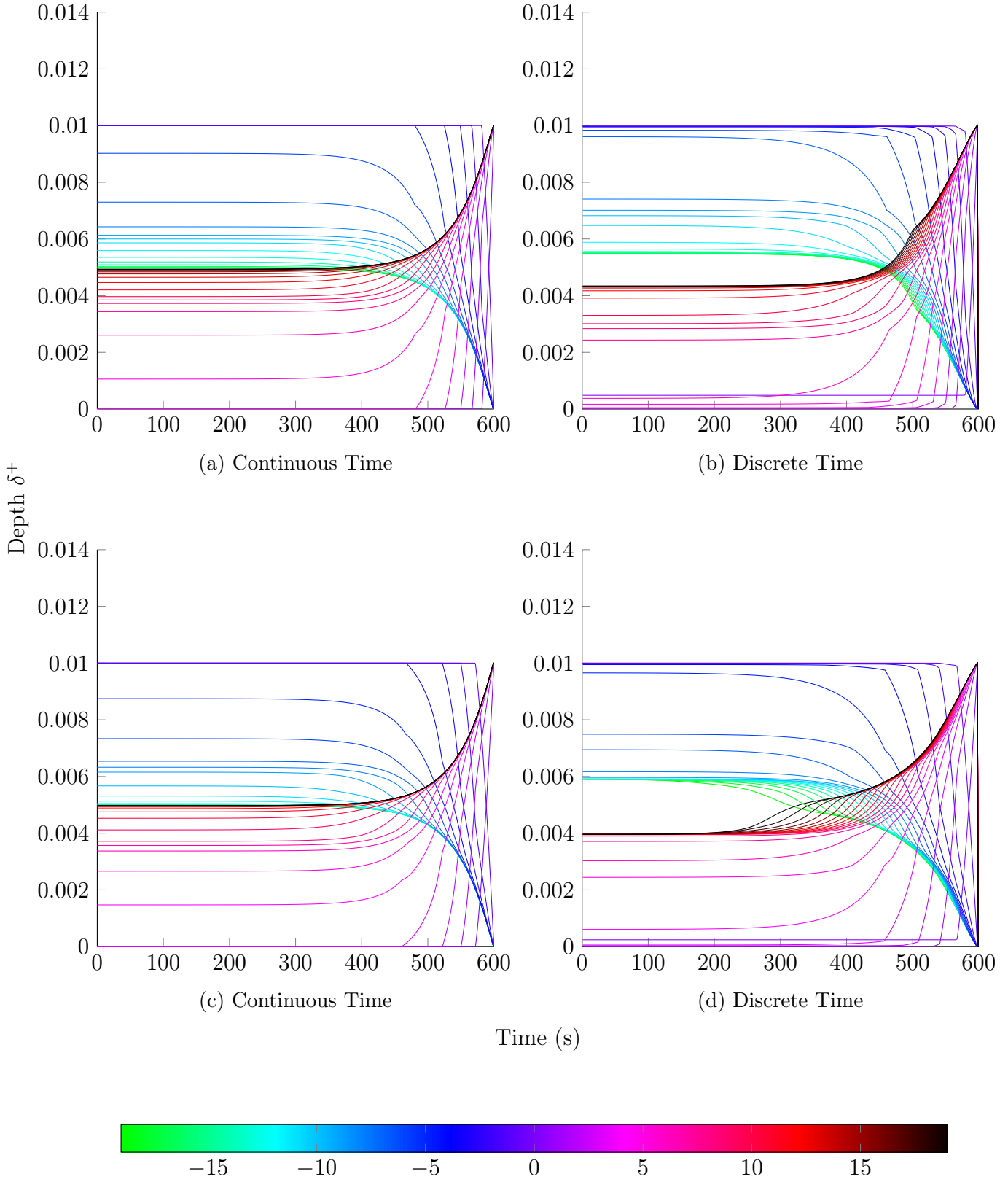
Figure 4.2: Optimal buy depths δ^+ for Markov state $Z = (\rho = 0, \Delta S = 0)$, implying neutral imbalance and no previous price change. We expect no change in midprice.
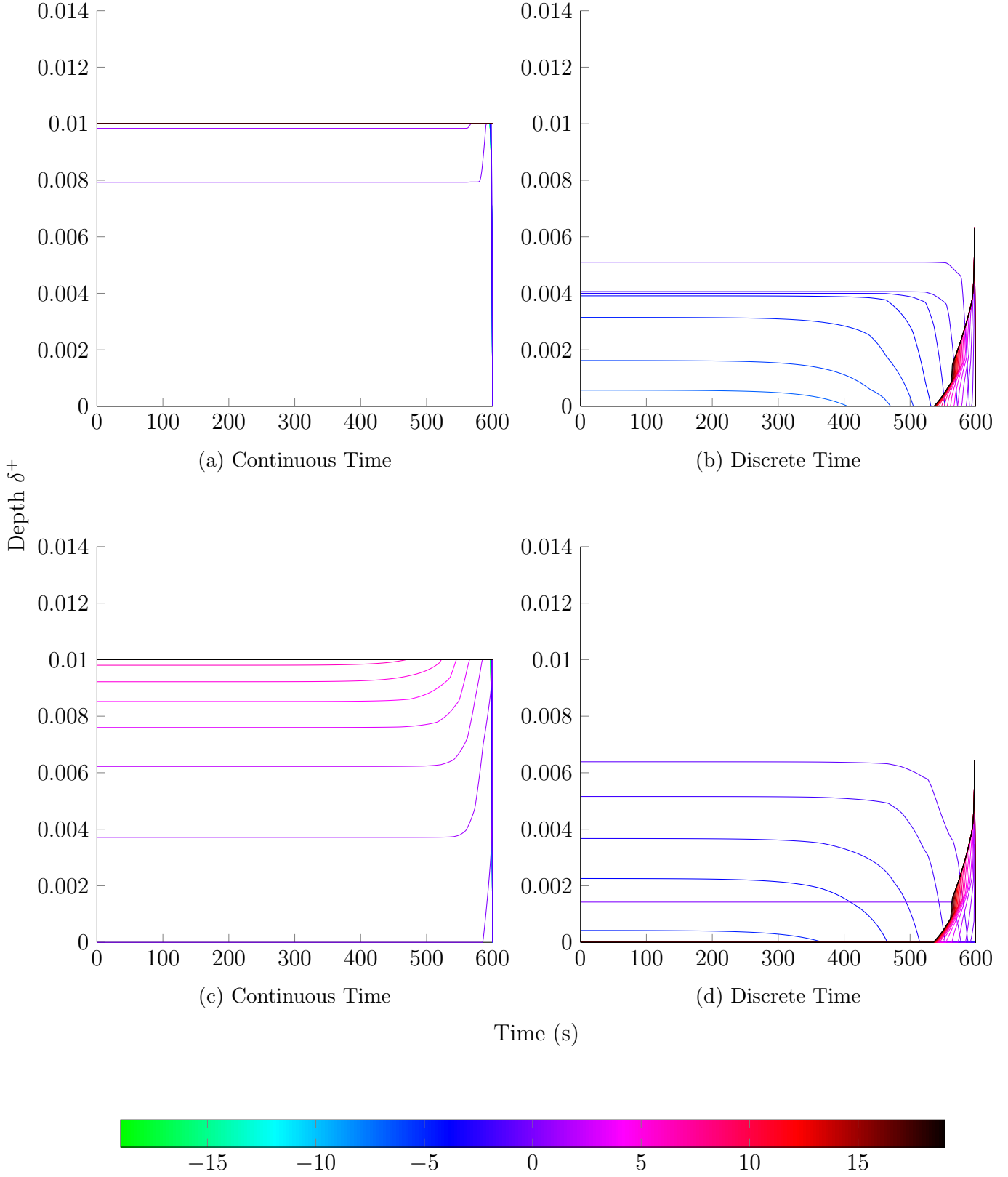
Figure 4.3: Optimal buy depths δ^+ for Markov state $Z = (\rho = +1, \Delta S = +1)$, implying heavy imbalance in favor of buy pressure, and having previously seen an upward price change. We expect the midprice to rise.

Markov State $Z = (-1, -1)$ (Figure 4.1)

Cts versus Cts w nFPC: For $q \geq 0$, both strategies post aggressive bid depths that suggest an inclination to buy. The nFPC strategy is less aggressive for $q < 0$, posting closer to zero depth only for larger short positions.

Dscr versus Dscr w nFPC: The behaviour of these two calibrations is very similar. Both models show a discontinuity in dynamics at $q = 0$, where at $q = -1$ it is posting at maximal depth, at $q = 0$ it jumps to approximately \$0.006, and at $q = 1$ again jumps lower. Otherwise, the nFPC strategy posts slightly more aggressively only when $q = 1$ or 2.

Cts vs Dscr: These models produce behaviours that are worlds apart. Whereas the Cts model seems to be saying that it wants to take this opportunity to go long, perhaps stocking up inventory while prices are low, the Dscr strategy suggests it's pulling out and avoiding purchasing.

Markov State $Z = (0, 0)$ (Figure 4.2)

Here we see near identical model behaviour. Similarities or correlations in backtesting performance can likely be attributed to this behaviour, as the majority of the day is spent in a Markov state for which $\Delta S = 0$, as seen here. (Recall that ρ, by contrast, is computed via evenly spaced percentiles symmetric around zero, so that time spent in each imbalance state is evenly distributed.)

Markov State $Z = (+1, +1)$ (Figure 4.3)

Cts versus Cts w nFPC: We see a nearly symmetric behaviour compared with the opposite Markov state. Here for $q \leq 0$, both strategies post maximal bid depths, suggesting a disinclination toward buying. The nFPC strategy is more aggressive for $q > 0$ and small inventory positions.

Dscr versus Dscr w nFPC: Again these calibrations yield very similar behaviours, and as in the Cts case, it is near opposite to what was seen in the opposite Markov state.

Cts vs Dscr: As before, these two models display near opposite behaviours between each other. The Dscr model is posting aggressive depths near zero in an attempt to purchase, while the Cts model is posting deeper into the book to avoid purchasing.

Finally, we note that we see relative stability in the posting depths at a time horizon of 600 seconds. This is consistent with the findings in Table 2.2, where we saw that the transition probability matrix $\boldsymbol{P}(t)$ converged for INTC to an error threshold of 10^{-10} within 771 timesteps of 1s each.

(a) Continuous Time

(b) Discrete Time

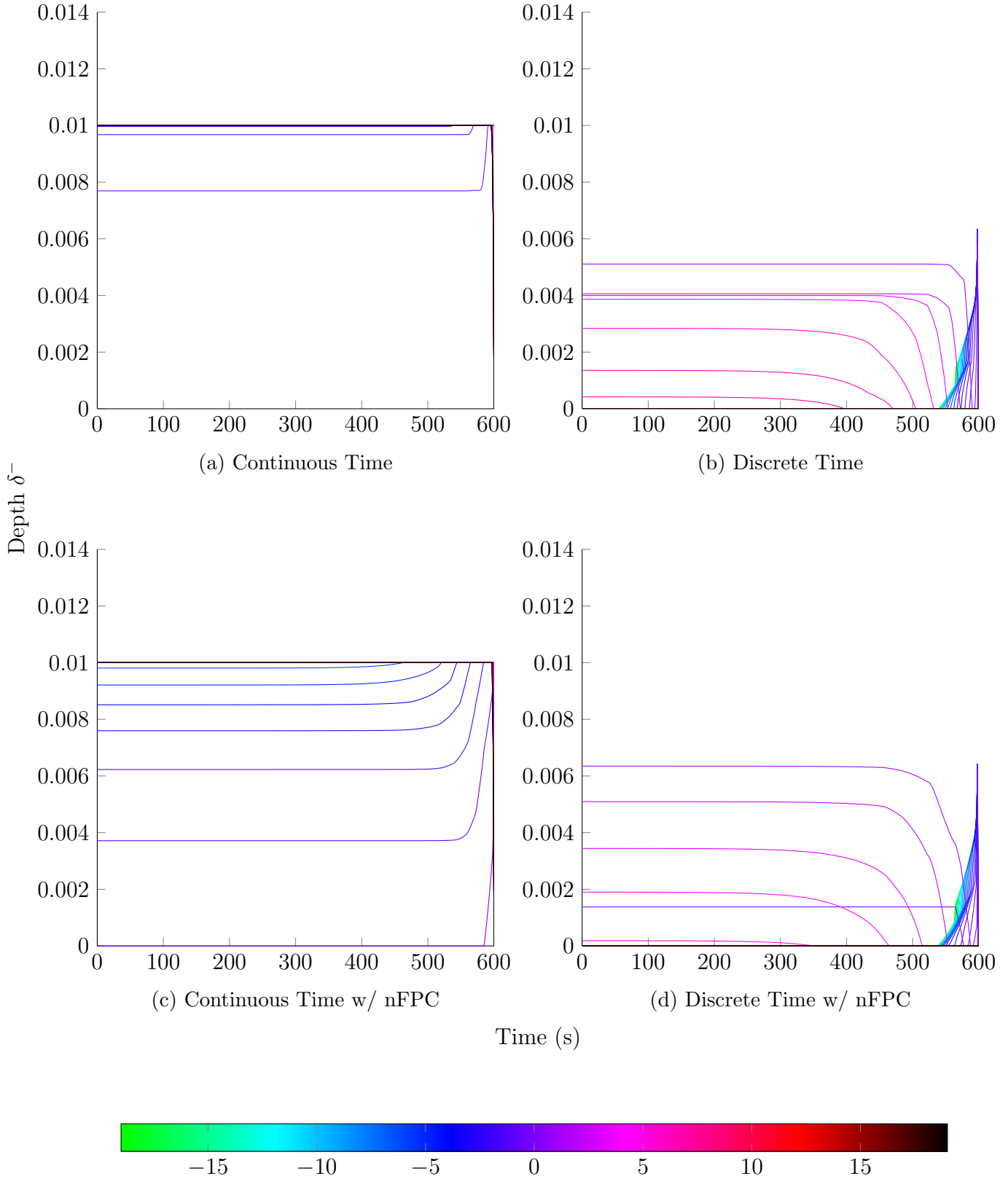(c) Continuous Time w/ nFPC

(d) Discrete Time w/ nFPC

Time (s)

Figure 4.4: Optimal sell depths δ^- for Markov state $Z = (\rho = -1, \Delta S = -1)$, implying heavy imbalance in favor of sell pressure, and having previously seen a downward price change. We expect the midprice to fall.
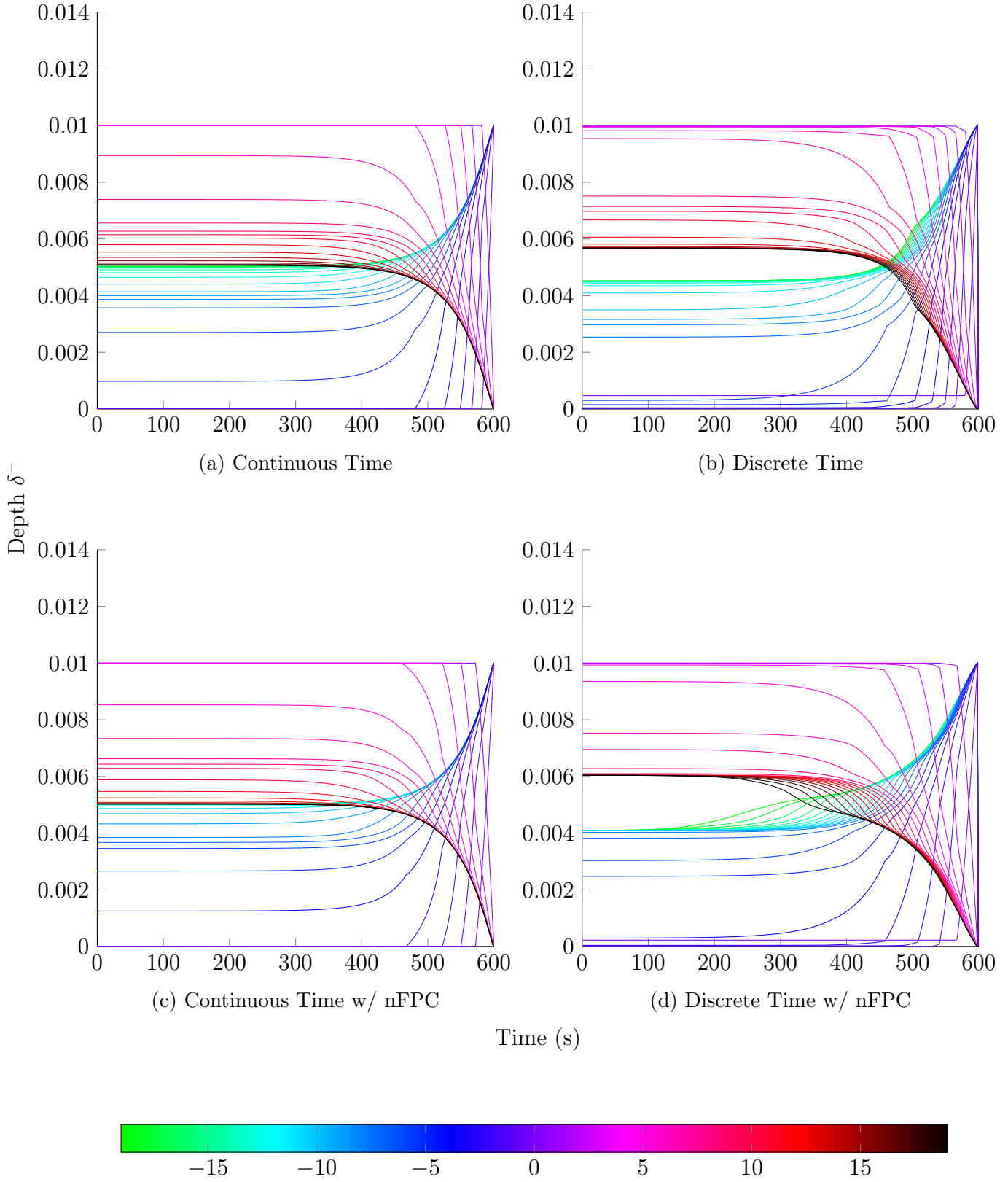
Figure 4.5: Optimal sell depths δ^- for Markov state $Z = (\rho = 0, \Delta S = 0)$, implying neutral imbalance and no previous price change. We expect no change in midprice.

63
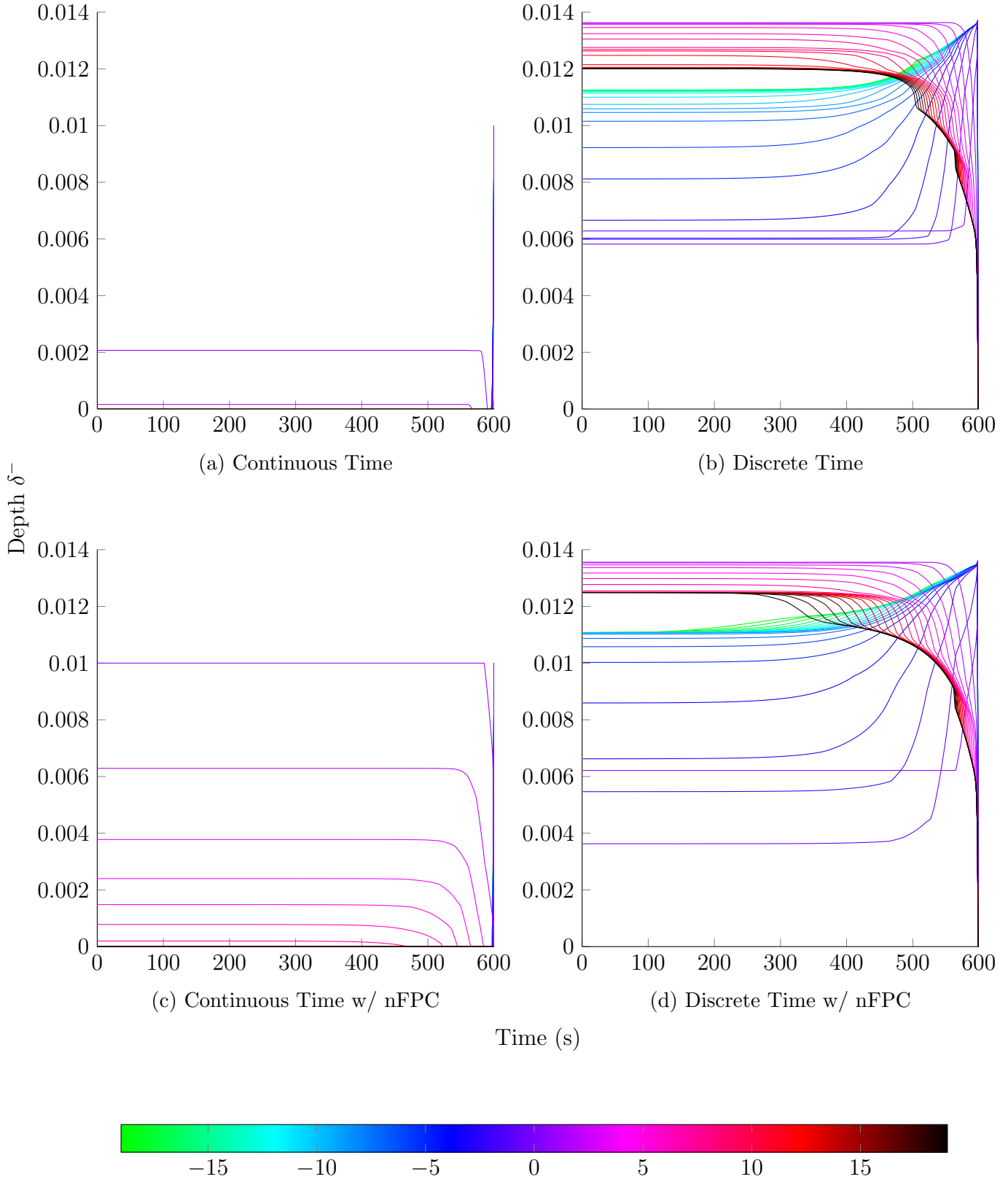
Figure 4.6: Optimal sell depths δ^- for Markov state $Z = (\rho = +1, \Delta S = +1)$, implying heavy imbalance in favor of buy pressure, and having previously seen an upward price change. We expect the midprice to rise.

4.2.1 Comparing Optimal Control Performance

In Figure 4.7a we plot the normalized PnL for the four strategies, calibrated and back-tested using data for `ORCL` from 2013-05-15. At a glance the four plots show obvious similarities in trajectory, as well as in the distinct spikes between 13h and 14.5h. Nevertheless the correlation of arithmetic returns, Table 4.1, shows that the strategies' returns were uncorrelated. Indeed, while the overall paths are similar, on close inspection the individual returns do show markedly different behavior.

	Cts	Cts w nFPC	Dscr	Dscr w nFPC
Cts	1.0000			
Cts w nFPC	-0.0109	1.0000		
Dscr	-0.0120	0.0122	1.0000	
Dscr w nFPC	-0.0015	0.0034	-0.0165	1.0000

Table 4.1: Correlation of returns

However, we find instead that the returns are co-integrated. On running the Engle-Granger cointegration test with statistics computed using an augmented Dickey-Fuller test of residuals, the τ-test and z-test both returned p-values of 0.001, thus rejecting the null hypothesis of no co-integration. Indeed, the co-integration relation plotted in Figure 4.8 displays stationarity, thus confirming the existence of a co-integration relation.
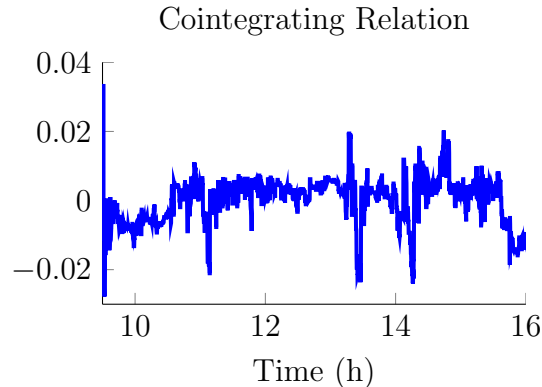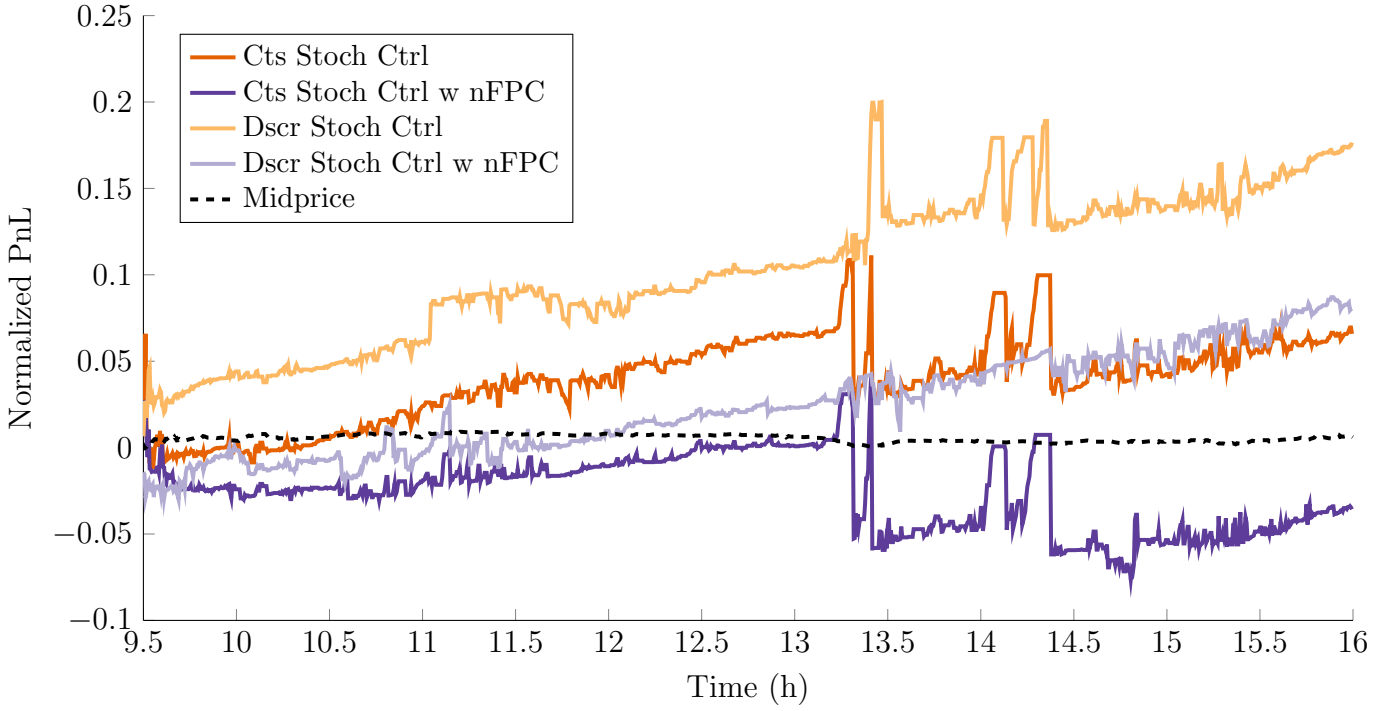

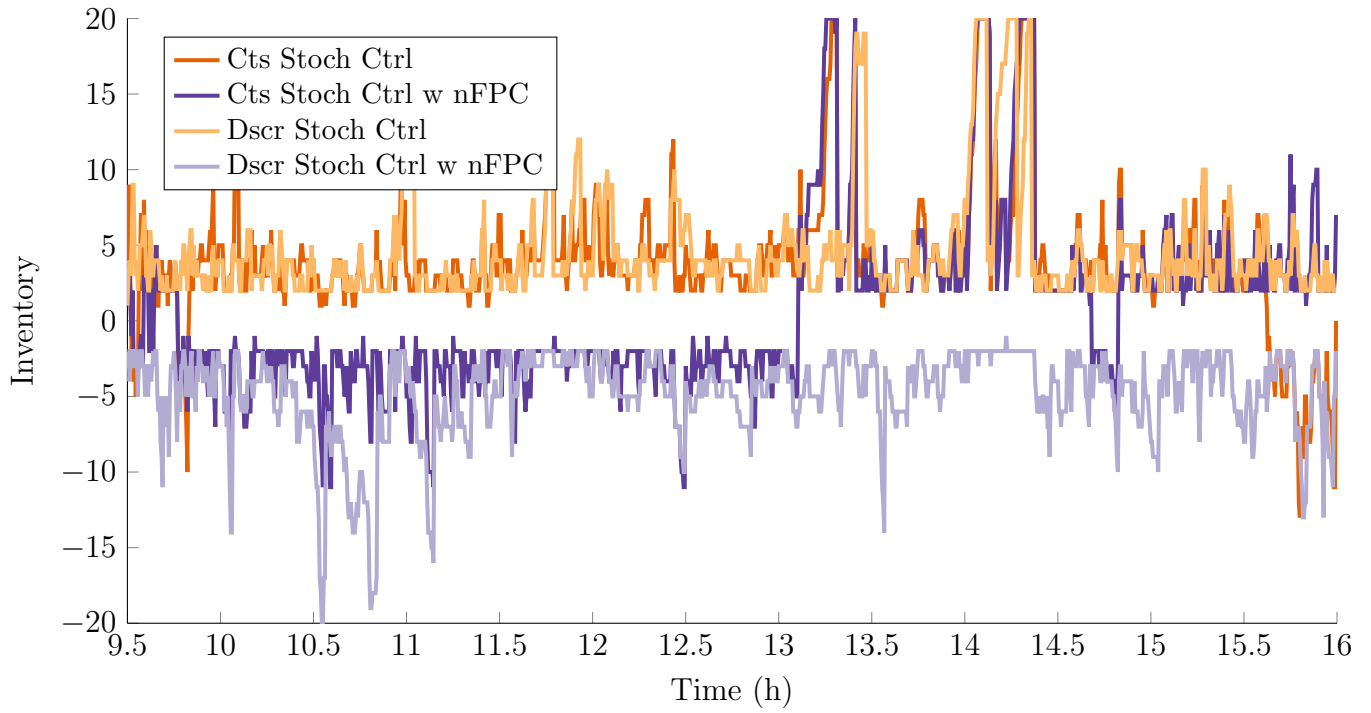Figure 4.8: Co-integration relation of the four stochastic control methods.

From the inventory plot in Figure 4.7b we see that the strategies always avoid maintaining

(a) Performance comparison of the four stochastic control methods.

(b) Inventory comparison of the four stochastic control methods.

Figure 4.7: Comparison of the four stochastic control methods.

	Market Orders	Limit Orders
Cts	536	1280
Cts w nFPC	1010	1306
Dscr	559	1285
Dscr w nFPC	523	1287

Table 4.2: Number of trades comparison of the four stochastic control methods.

zero inventory. This is not surprising: in both the discrete and continuous cases we found that the value function ansatz $h(t, z, q)$ was non-negative, and was equal to zero at zero inventory. The interpretation is that there is no added value to having zero inventory, whereas non-zero inventory can at worst have zero value. Thus it is always profitable, from a value-function standpoint, to have non-zero inventory. Further, we see that the strategies rarely cross the zero-inventory barrier. This is likely attributed to the backtesting algorithm itself, which gives priority to executing buy market orders above sell market orders - we suspect that once the strategy gets into either positive or negative inventory territory, the ansatz function h rarely produces the circumstances to cross the inventory sign barrier by virtue of the non-linear mark-to-market behavior on either side of zero inventory.

Concerning trade execution, the number of executed market orders and filled limit orders generated by each strategy are presented in Table 4.2. The surge in market orders seen for the Cts w nFPC strategy can be explained by the difference in the $\delta^{\pm}$ plots. As mentioned already, from the stochastic analysis chapter, we know that if $q < 0$ and $\delta^+ = 0$, or if $q > 0$ and $\delta^+ = 1/\kappa$, then we execute a buy MO. Likewise, if $q < 0$ and $\delta^- = 1/\kappa$, or if $q > 0$ and $\delta^- = 0$, then we execute a sell MO. In Figure 4.1 we see that we have $\delta^+ = 0$ for almost all inventory values, and in Figure 4.3 we have $\delta^+ = 1/\kappa$ for almost all inventory values. This tells us that when the Markov chain state is in one of the non-neutral states, the Cts w nFPC strategy will execute market orders when possible, as it expects prices to move in the corresponding direction. Regarding overall number of trades, it should be noted that we did not include the cost of market order execution in the stochastic control problem. Thus, actual performance would have been negatively affected in proportion to the number of market orders listed.

To better see how the strategies differ in behaviour, in the figures that follow we show a short sample path on a fine timescale spanning about 2 minutes. In Figure 4.9 we plot the midprice path (black line), the optimal posting depths on either side of the real

bid/ask prices (gray lines), our execution of market orders (dark blue and dark green), and track incoming external market orders (light blue and light green) that either fill our limit orders (solid lines) or do not (dashed lines). Figure 4.10 plots just the optimal depths as they react to the changing Markov state, allowing a better comparison of the behaviours, as well as highlighting the almost-symmetric behaviour between δ^+ and δ^-. Figure 4.11 and Figure 4.12 show the effect on PnL and inventory, respectively.

Figure 4.9: Sample paths of the optimal trading strategies, showing price, limit order posting depths, executed market orders, and filled limit orders.

Figure 4.10: Sample paths of the optimal trading strategies, showing price, limit order posting depths, executed market orders, and filled limit orders.
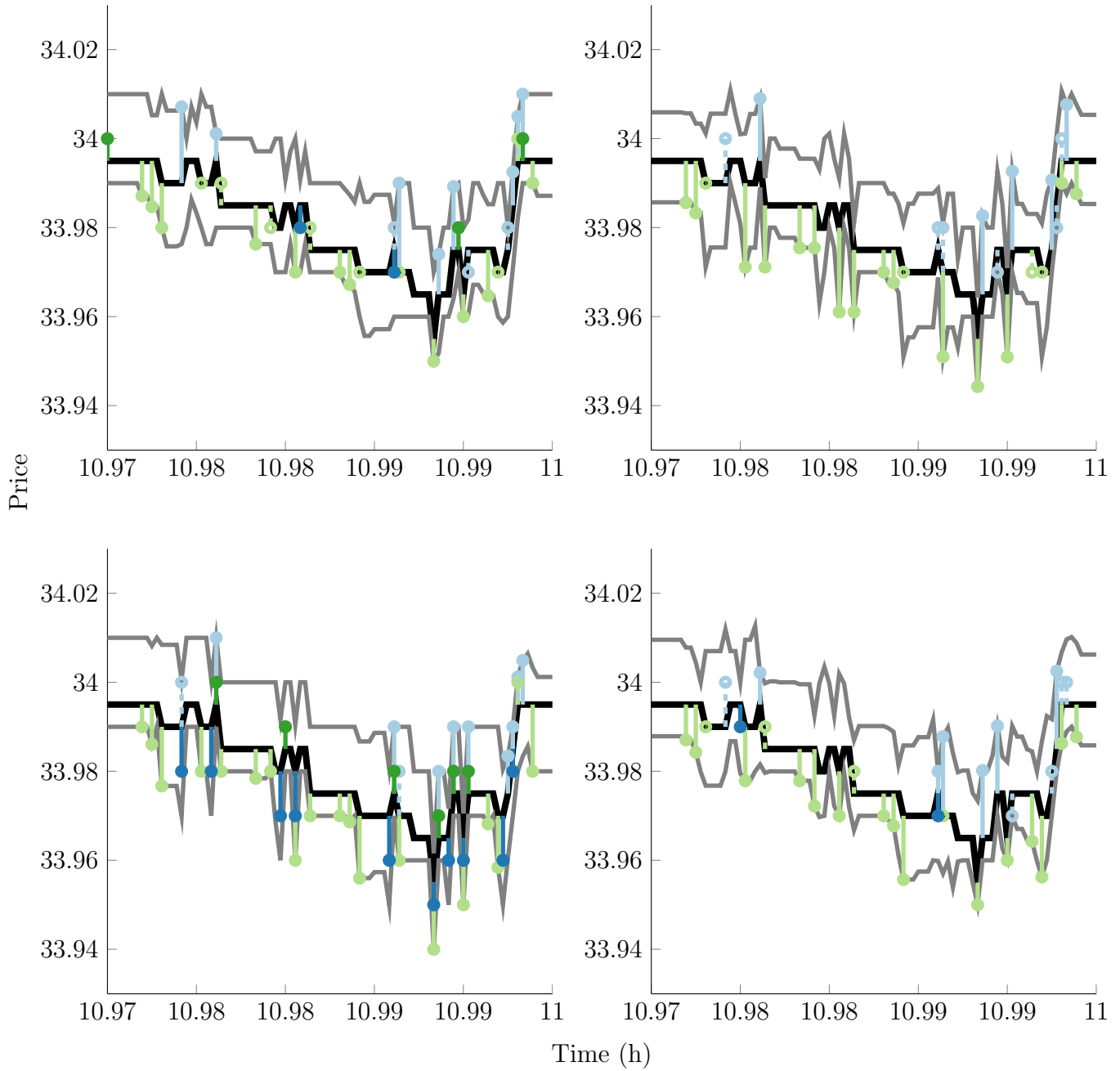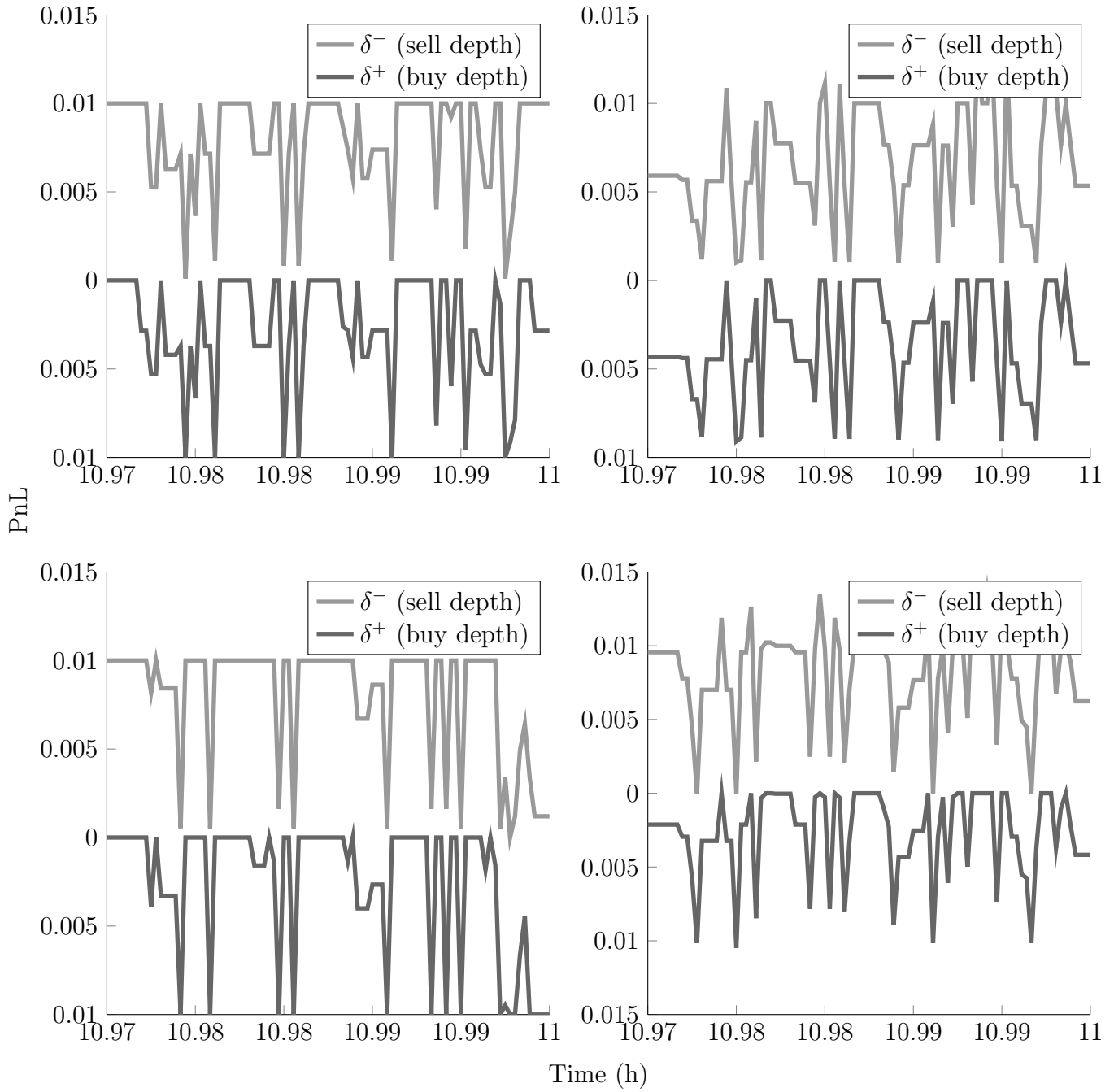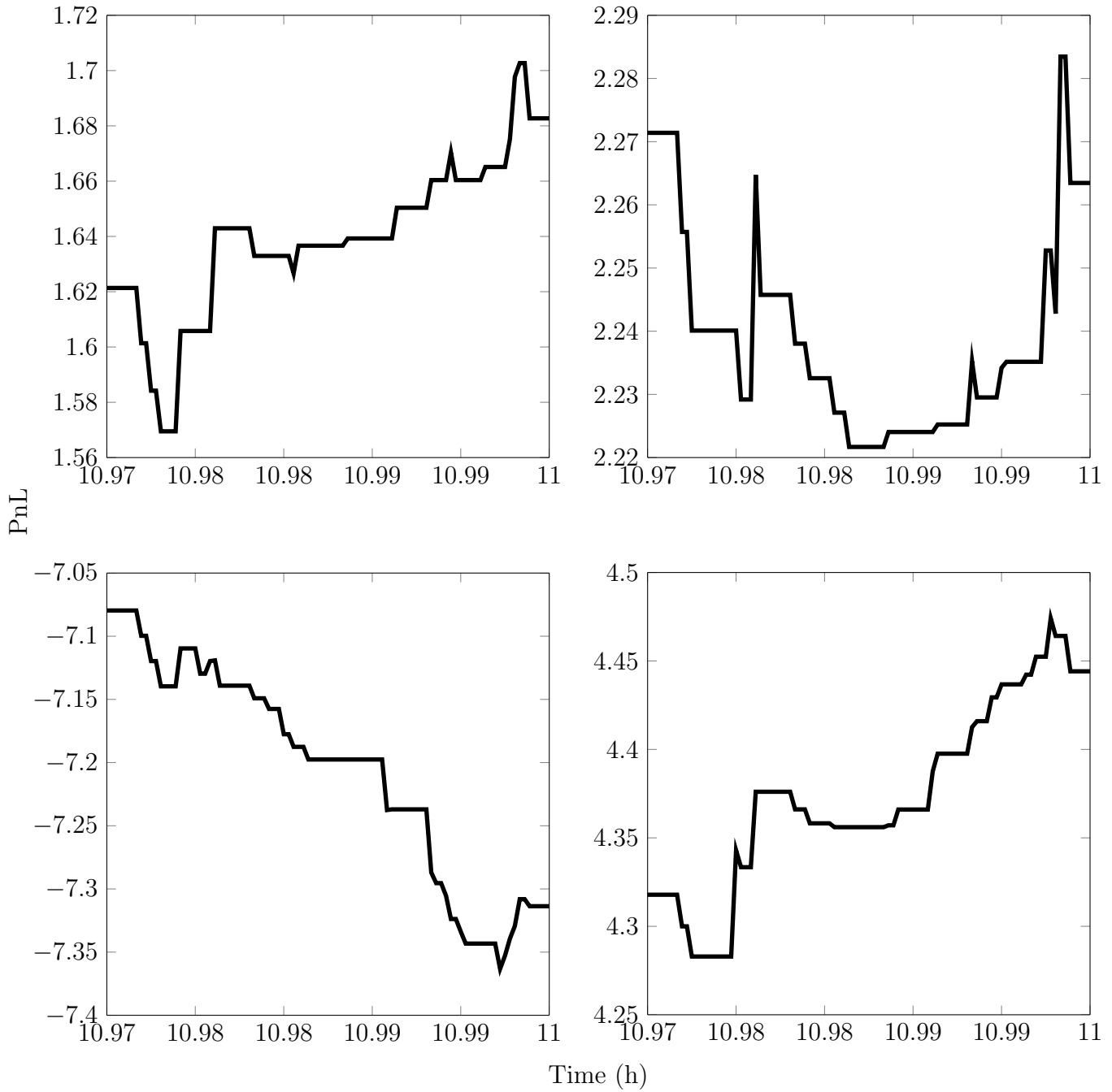
Figure 4.11: Sample paths of the optimal trading strategies, showing price, limit order posting depths, executed market orders, and filled limit orders.
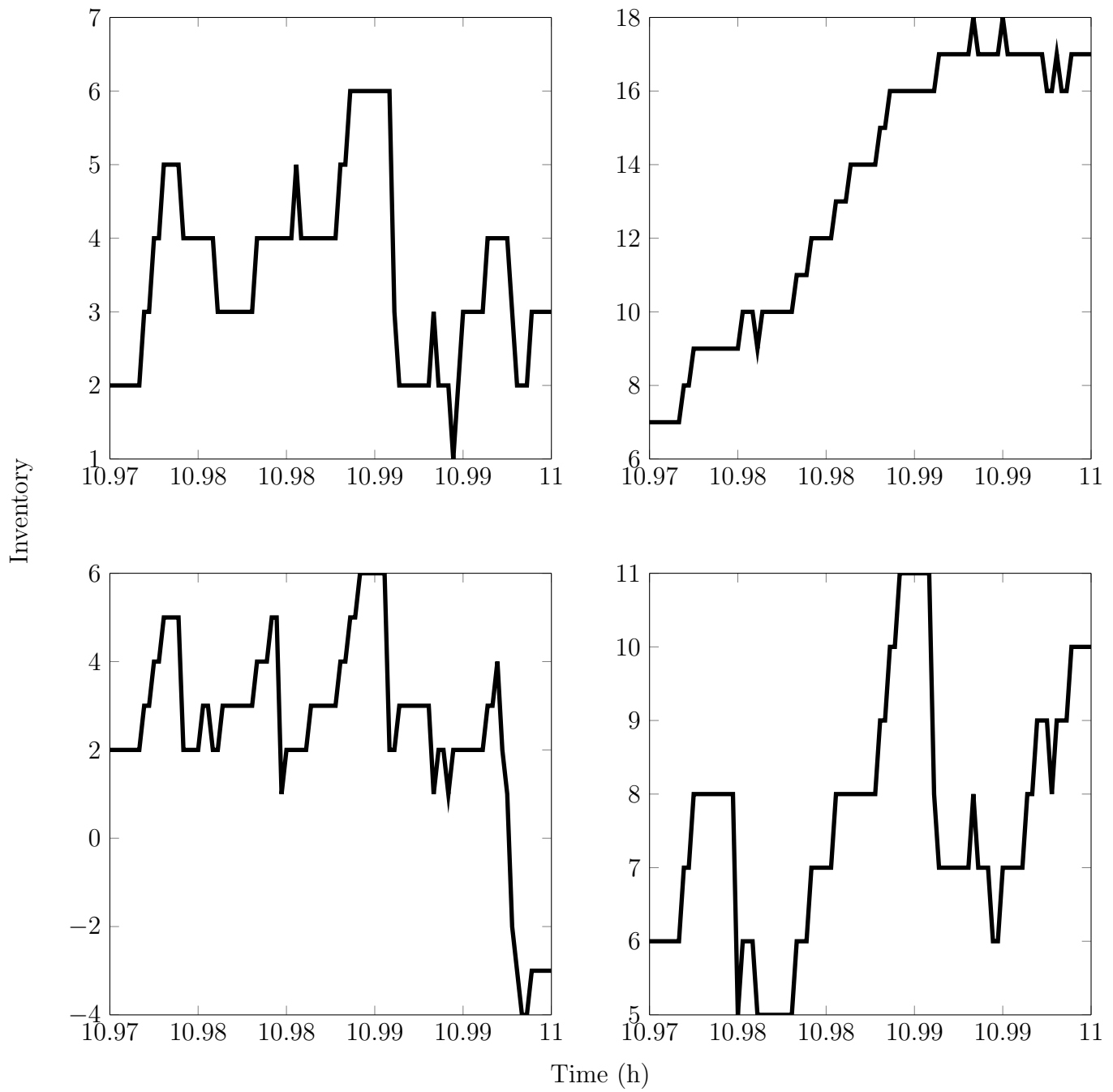
Figure 4.12: Sample paths of the optimal trading strategies, showing price, limit order posting depths, executed market orders, and filled limit orders.

4.3 In-Sample Backtesting

4.3.1 Same-Day Calibration

We begin our in-sample backtesting same-day calibration: calibration was run for each ticker and each trading day of 2013, and backtesting was then done for each strategy using the same day's calibration. Each backtest would yield the end of day PnL, average inventory held during the day, and the number of executed market orders and filled limit orders. In Table 4.3 we show performance values for several metrics of interest, while Figure 4.13 compares the day-over-day performance of the various strategies.

Since we are calibrating and backtesting using the same underlying data, the calibration should be best attuned to the price dynamics for that praticular day, and hence we expect the performance using same-day calibration to exceed that of the weekly offset calibration and the annual calibration (detailed in the sections that follow). Looking at the % Win column in Table 4.3 we see that trading on `FARO` very rarely produces positive PnL. This is not surprising and was mentioned at the conclusion of the exploratory data analysis chapter: `FARO` is highly illiquid, with daily volume hovering around 200k, and its bid-ask spread averages approximately 20 cents. This makes it never profitable to execute market orders (due to crossing the spread), and because our optimal strategies still force us to post limit orders at depths between 0 and $1/\kappa = 0.01 = 1$cent, the most probable occurrence is that our limit orders are lifted adversely. `NTAP` seems to be a borderline case for liquidity, with average volumes around 4m, and here the strategies exhibit weak regularity of profits. The most liquid stocks, `ORCL` and `NTAP`, with average volumes around 15m and 30m respectively, post extremely promising results: the stochastic control strategies produce positive EOD PnL more than 90% of the time. The discrete time controller outperforms its continuous time counterpart, and in particular we highlight that in the case of `INTC`, we attain a very good Sharpe ratio of 2.5.
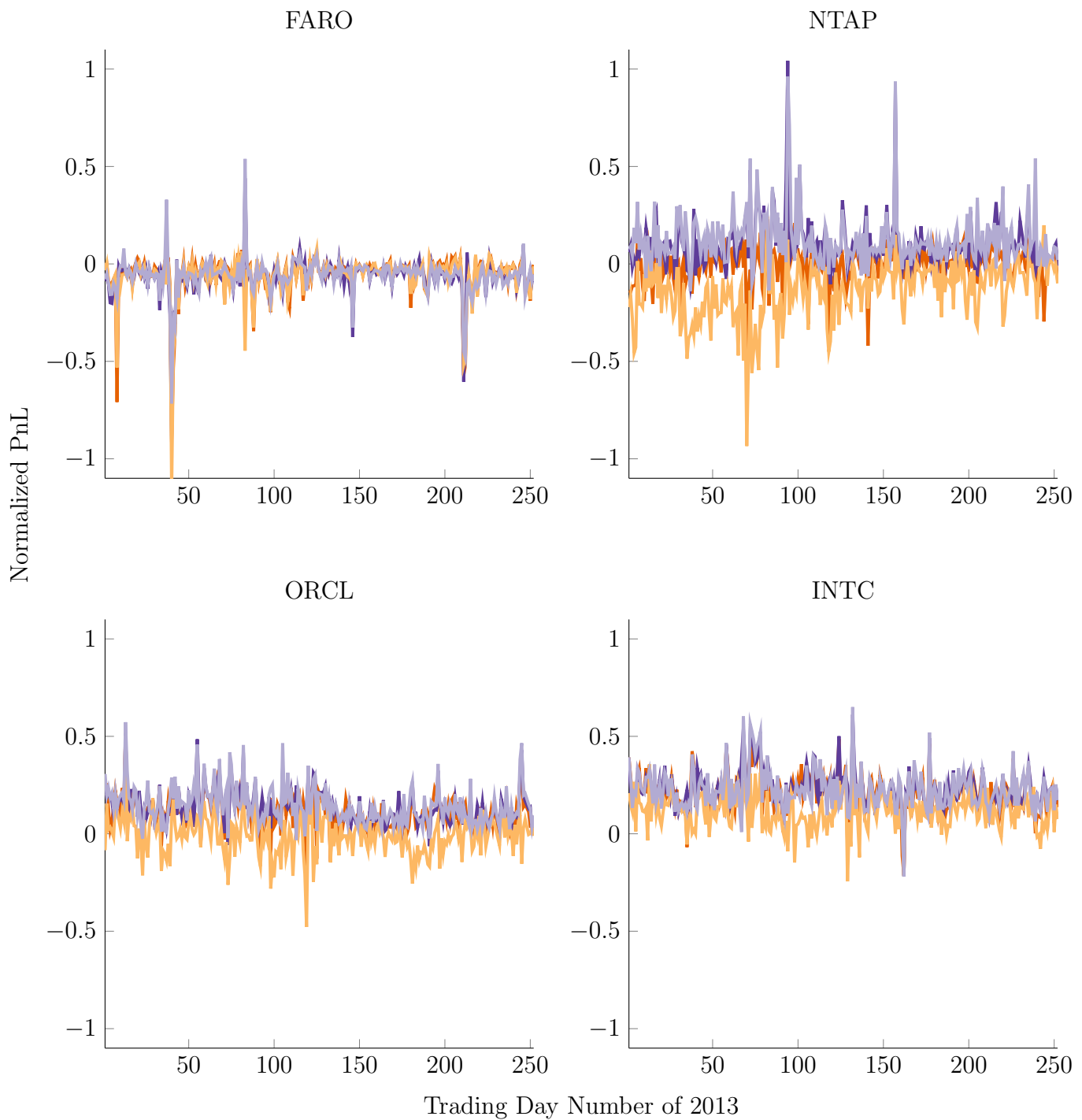
Figure 4.13: End of day strategy performances: in-sample backtesting using same-day calibration.

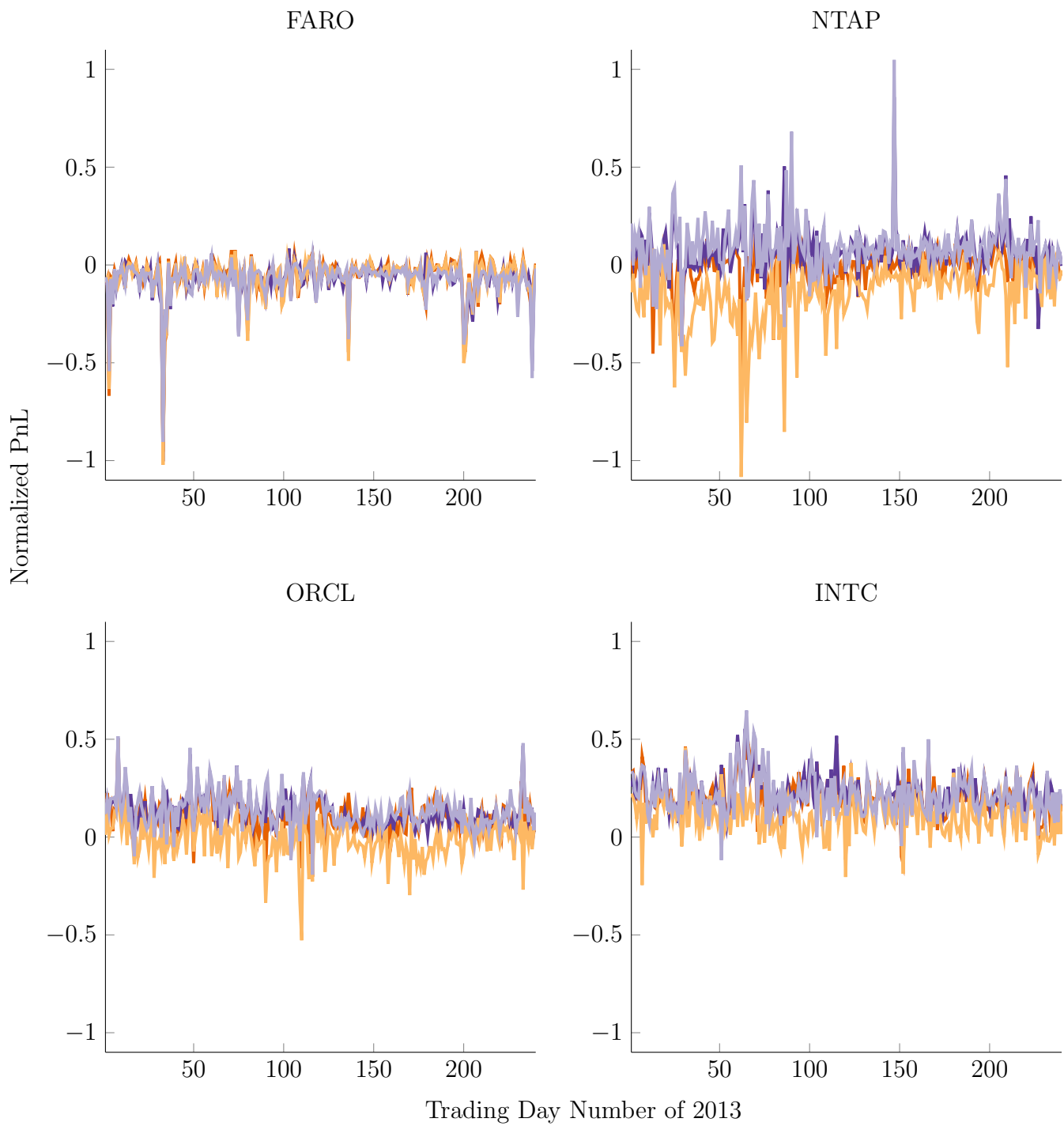| Strategy	Return	Sharpe	Trades	Inv	% Win	Max Loss	Max Win
FARO							
Naive	-0.879	-0.808	413	0.47	0.07	-7.109	5.715
Naive+	0.101	0.107	213	2.45	0.74	-8.797	5.336
Naive++	0.002	0.021	7	0.17	0.50	-0.842	0.320
Cont	-0.059	-0.551	201	0.09	0.18	-0.912	0.071
Dscr	-0.064	-0.695	210	-0.02	0.08	-0.914	0.440
Cont w nFPC	-0.063	-0.571	204	0.08	0.14	-1.161	0.077
Dscr w nFPC	-0.060	-0.662	209	-0.03	0.09	-0.716	0.539
NTAP							
Naive	-0.188	-0.316	842	-9.81	0.23	-3.238	3.524
Naive+	0.388	0.169	3562	-9.73	0.74	-19.367	10.201
Naive++	-0.005	-0.012	157	-0.90	0.54	-2.888	2.558
Cont	-0.006	-0.062	2265	0.40	0.56	-0.441	0.215
Dscr	0.099	0.767	1872	4.74	0.86	-0.126	1.042
Cont w nFPC	-0.141	-0.951	2897	0.65	0.14	-0.935	0.244
Dscr w nFPC	0.121	0.881	1738	2.82	0.89	-0.139	0.962
ORCL							
Naive	-0.105	-0.253	484	1.40	0.28	-1.837	2.180
Naive+	-0.034	-0.011	4086	-55.18	0.61	-17.501	18.400
Naive++	0.002	0.006	132	0.61	0.52	-0.798	2.636
Cont	0.115	1.348	1874	1.94	0.92	-0.217	0.521
Dscr	0.135	1.620	1898	3.93	0.98	-0.063	0.515
Cont w nFPC	-0.010	-0.100	2455	1.32	0.48	-0.478	0.503
Dscr w nFPC	0.144	1.501	1759	2.85	0.97	-0.032	0.573
INTC							
Naive	-0.082	-0.228	258	-5.21	0.33	-1.465	1.425
Naive+	0.365	0.134	3962	-32.50	0.63	-11.202	11.669
Naive++	-0.001	-0.003	74	-0.84	0.48	-1.314	1.264
Cont	0.214	2.159	1577	5.17	0.97	-0.213	0.487
Dscr	0.232	2.528	1642	4.48	0.98	-0.217	0.611
Cont w nFPC	0.114	1.218	1894	2.01	0.90	-0.244	0.416
Dscr w nFPC	0.226	2.202	1569	4.28	0.98	-0.220	0.650

Table 4.3: Averaged strategy performance results: in-sample backtesting using same-day calibration.

4.3.2   Week Offset Calibration

The next type of in-sample backtesting done was to calibrate for each ticker and each trading day of 2013, and to use the results to backtest on the date given by the calibration date shifted forward 7 days. Thus, the calibration obtained on Monday, January 2, 2013 would be used to backtest on Monday, January 9, 2013. Performance values are given in Table 4.4, and Figure 4.14 compares the day-over-day performance of the various strategies.

Most of the observations from the previous section apply here. Chiefly, the illiquid stock FARO produces negative PnL and the low-liquidity stock NTAP approximately breaks even. As expected, the week offset calibration underperforms same-day calibration, but remarkably the difference is very small: in the case of INTC, the discrete time controller still generates a Sharpe ratio of approximately 2.5, and in this case only returned negative PnL once during the trading year.

The similarity of the results can be interpreted in several ways. First, it is possible that trading behaviour is stable across days of the week, such that substituting one Monday for another yields a similar calibration. This is readily testable by calibrating on a given day and backtesting on the subsequent trading day, instead of a one-week offset. On the other hand, even with dissimilar data, it's possible that the calculation of $\delta^{\pm}$ is stable with respect to day-over-day fluctuations of data.

Figure 4.14: End of day strategy performances: in-sample backtesting using a one-week offset for calibration.

Strategy	Return	Sharpe	# MO	# LO	Inv	% Win	Max Loss	Max Win
FARO								
Naive	-1.072	-0.444	435	0	1.74	0.08	-34.276	2.984
Naive+	0.045	0.046	0	213	2.26	0.74	-8.764	5.363
Naive++	-0.003	-0.027	0	6	0.25	0.50	-1.138	0.444
Cts	-0.060	-0.565	53	149	0.08	0.20	-0.955	0.077
Dscr	-0.076	-0.764	80	133	-0.07	0.07	-1.004	0.084
Cts w nFPC	-0.065	-0.590	56	149	0.09	0.17	-1.022	0.072
Dscr w nFPC	-0.076	-0.778	78	133	0.07	0.07	-0.904	0.053
NTAP								
Naive	-0.303	-0.316	854	0	-10.96	0.20	-9.463	4.349
Naive+	0.290	0.122	0	3537	-13.83	0.73	-19.806	10.266
Naive++	-0.048	-0.084	0	156	-1.79	0.52	-6.310	2.670
Cts	-0.016	-0.165	830	1405	0.37	0.52	-0.612	0.158
Dscr	0.070	0.593	460	1388	5.06	0.79	-0.355	0.858
Cts w nFPC	-0.156	-0.987	1506	1425	0.70	0.09	-1.083	0.106
Dscr w nFPC	0.091	0.656	332	1401	3.16	0.85	-0.416	1.048
ORCL								
Naive	-0.112	-0.248	492	0	3.66	0.28	-3.197	2.452
Naive+	0.066	0.022	0	4049	-50.06	0.64	-17.396	18.873
Naive++	0.002	0.005	0	134	0.64	0.49	-1.691	2.537
Cts	0.098	1.181	545	1318	1.86	0.90	-0.203	0.310
Dscr	0.126	1.547	578	1310	4.01	0.97	-0.097	0.505
Cts w nFPC	-0.013	-0.130	1069	1365	1.39	0.47	-0.528	0.500
Dscr w nFPC	0.135	1.459	416	1338	3.16	0.96	-0.192	0.516
INTC								
Naive	-0.057	-0.179	274	0	-3.63	0.31	-0.954	1.766
Naive+	0.375	0.138	0	3925	-25.43	0.65	-11.060	11.465
Naive++	0.013	0.055	0	77	-0.47	0.53	-1.815	1.126
Cts	0.202	1.995	423	1139	4.76	0.98	-0.139	0.513
Dscr	0.226	2.494	501	1136	4.62	0.99	-0.029	0.560
Cts w nFPC	0.107	1.111	681	1187	1.64	0.87	-0.245	0.457
Dscr w nFPC	0.215	2.027	401	1156	3.78	0.99	-0.118	0.647

Table 4.4: Averaged strategy performance results: in-sample backtesting using a one-week offset for calibration.

4.3.3 Annual Calibration

The second type of out-of-sample backtesting done was to calibrate using data amalgamated from the entire 2013 trading year. This was a very rich calibration source, as it effectively ensured that every possible state of the Markov chain would have had sufficient observations. Further, this caused us to fix the imbalance bins ρ for the entire year, rather than having bins (and hence what it means to be 'heavy buy imbalance' and 'neutral imbalance') vary each day. Performance values are given in Table 4.5, and Figure 4.15 compares the day-over-day performance of the various strategies.

Here we backtest only the more liquid of the stocks, ORCL and INTC. In comparing Table 4.5 with Table 4.4, we note some interesting observations. Again we see the most liquid stock, INTC, posting on average the better results using the strategies, suggesting that using a liquid stock is key. (INTC started the year at \$21.38 and gained 21.42% over the year, while ORCL started at \$34.69 and climbed 10.29%. However, NTAP started at \$34.30 and gained 19.94%, similar in performance to INTC, and yet performed substantially worse.) Whereas we have seen thus far that the nFPC strategies underperform the regular calibration, here the roles were reversed in terms of performance, number of market orders used, and average inventory held. Across the strategies we see stability in the number of limit orders used, which suggests that this isn't so much strategy dependent as it is externally dependent on outside agents submitting their market orders. In the case of ORCL we see that the Cts Stoch Ctrl strategy was particularly susceptible to the sharp downward spikes on days 55, 100, and 119, which corresponded to large sell-offs in the market.
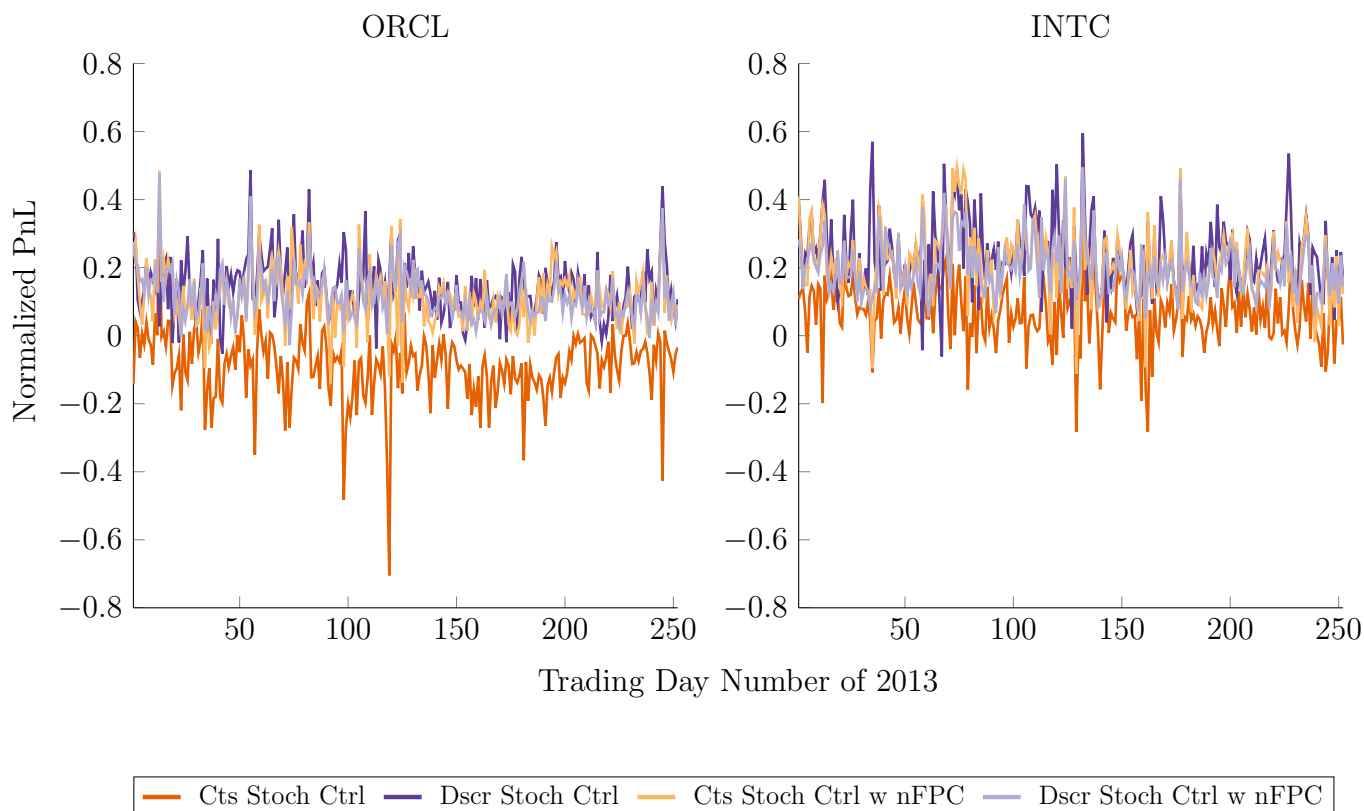
Figure 4.15: End of day strategy performances: in-sample backtesting on 2013 data, using amalgamated annual 2013 data for calibration.

Strategy	Return	Sharpe	# MO	# LO	Inv	% Win	Max Loss	Max Win
ORCL								
Cts	-0.089	-0.875	1540	1383	1.19	0.14	-0.705	0.393
Dscr	0.140	1.596	368	1344	0.46	0.96	-0.088	0.487
Cts w nFPC	0.113	1.327	476	1338	2.67	0.94	-0.140	0.484
Dscr w nFPC	0.118	1.735	590	1337	3.43	0.99	-0.028	0.474
INTC								
Cts	0.065	0.743	888	1207	1.22	0.84	-0.282	0.341
Dscr	0.235	2.189	380	1170	1.19	0.99	-0.061	0.595
Cts w nFPC	0.209	2.030	396	1160	5.58	0.98	-0.112	0.494
Dscr w nFPC	0.197	2.588	576	1164	3.78	1.00		0.490

Table 4.5: Averaged strategy performance results: in-sample backtesting on 2013 data, using amalgamated annual 2013 data for calibration.

4.4 Out-of-Sample Backtesting

From the in-sample backtesting we draw several conclusions:

- underlying stocks need to be highly liquid;

- underlying stocks need to have the smallest possible bid-ask spread;

- calibrating over a larger period of time produces comparable returns and slightly improved Sharpe ratios, and is therefore preferred;

- there is no clear victor between regular calibration and the nFPC method.

For out-of-sample backtesting we move to using 2014 data that has hitherto remained untouched. We elect to test all four strategies on two stocks, `INTC` and `AAPL`, that have average daily trading volumes of 30m and 45m respectively, and each have a typical bid-ask spread of the minimum 1 cent. `AAPL` underwent a 7-for-1 stock split on 2014-06-09, and prices are adjusted correspondingly in the underlying data; although prior to the split the bid-ask spread was an order of magnitude greater than 1 cent, we retain the 1 cent spread assumption on the adjusted pre-split prices to stay consistent with what was observed after the split. Additionally, we use a sliding calibration window of 1 month (21 trading days) and thus begin trading on the 22nd trading day of the year.

The results in Table 4.6 show the incredible out-of-sample results. The strategies post very solid returns and Sharpe ratios, and provide positive returns on almost every day that was tested. The strategies were run assuming our trade volume was 1 stock for every market order or limit order executed. Thus, to quantify these results in dollar terms, we can do a back of the envelope calculation by assuming for each of the 249 trading days of 2014, we trade 100 shares at a time, and multiply the average return (0.4 and 0.7 for `INTC` and `AAPL`, respectively) by the average share price during the year ($30 and $95, respectively). Thus, we conclude:

<div align="center">

Trading `INTC` would have generated revenue of $298,800.

Trading `AAPL` would have generated revenue of $1,655,850.

</div>

The capital requirements would have been the full price of the shares, $30 and $100 each, multiplied by the maximum long/short inventory of 20×100 shares - thus $260,000. This
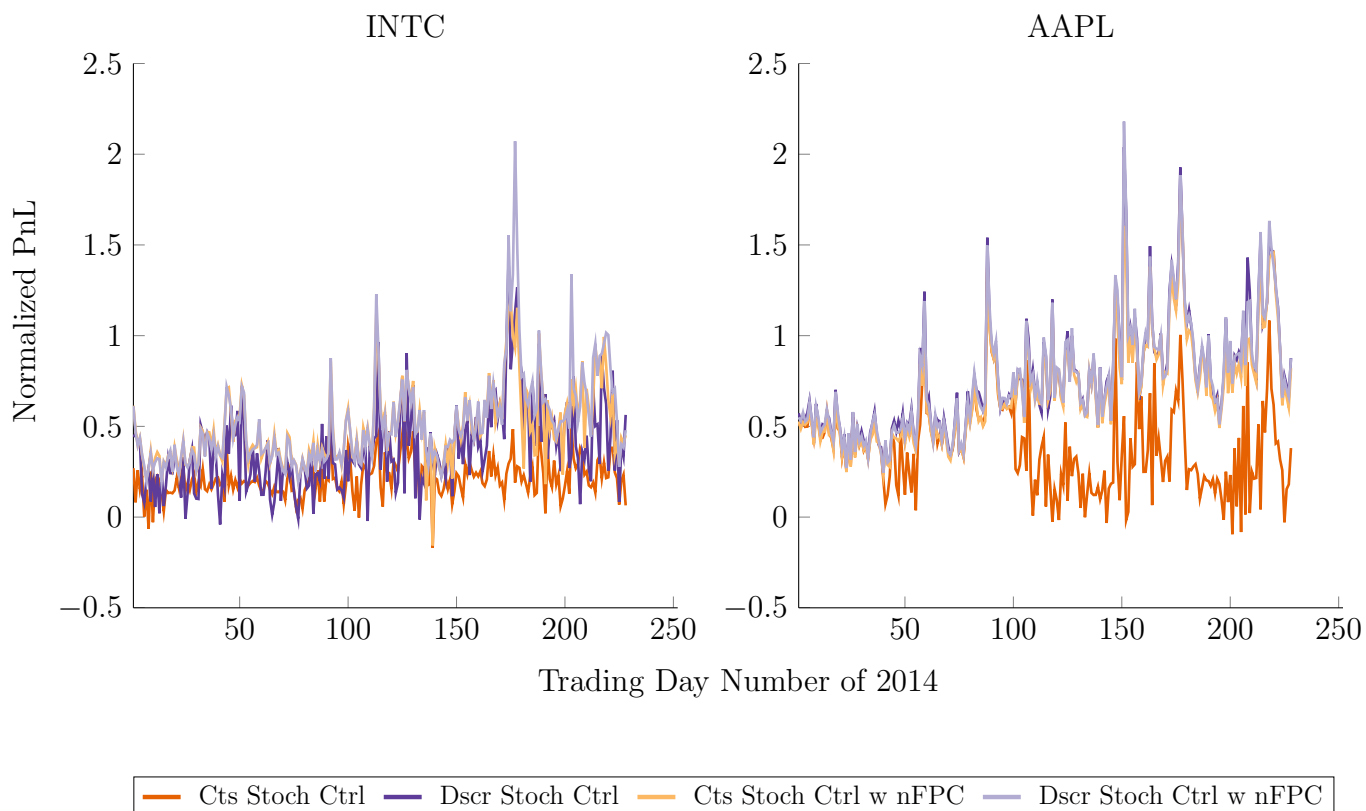
Figure 4.16: End of day strategy performances: out-of-sample backtesting on 2014 data, using amalgamated annual 2013 data for calibration.

Strategy	Return	Sharpe	# MO	# LO	Inv	% Win	Max Loss	Max Win
INTC								
Cts	0.209	2.112	2118	1758	0.44	0.98	-0.169	0.502
Dscr	0.372	1.591	949	1770	-5.89	0.98	-0.041	1.418
Cts w nFPC	0.483	2.364	704	1693	1.46	1.00	-0.156	1.194
Dscr w nFPC	0.515	2.033	490	1629	2.81	1.00		2.072
AAPL								
Cts	0.378	1.571	3853	6297	-5.80	0.96	-0.094	1.392
Dscr	0.761	2.457	830	5566	4.05	1.00		2.039
Cts w nFPC	0.710	2.479	1276	5689	2.93	1.00		1.803
Dscr w nFPC	0.764	2.442	796	5559	3.85	1.00		2.180

Table 4.6: Averaged strategy performance results: out-of-sample backtesting on 2014 data, using amalgamated annual 2013 data for calibration.

represents both a compound annual growth rate (CAGR) and return on investment (ROI) of 652%.

Chapter 5

Conclusion

5.1   Summary and Future Work

The backtesting results indicate that implementing the stochastic strategies on just two stocks would have generated a 652% return on investment in 2014. In addition, however, recurring fees would have included the co-location fees of storage rental and a cross-link to the exchange, approximately \$15,000 per month, and a subscription to the ITCH feed as well as access to NASDAQ's order submission protocol, another \$15,000 per month. Considering that there are other highly liquid shares with small bid-ask spreads listed on the NASDAQ such as `DELL` or `MSFT`, of which some may produce similar backtesting results, all signs point to the stochastic strategies being effective and worth taking to market.

Of course, this is a major oversimplification of reality. There are a number of assumptions and modelling choices that were made over the course of this research that must first be revisited prior to attempting forward performance testing (paper trading), let alone taking the system live. In what follows, I address what I consider to be the critical items among the list.

Market order costs.   Perhaps the easiest change of all, the dynamic programming equations need to account for the fact that market order executions come with a cost from the exchange, as they are essentially taking away liquidity. (Posting, modifying, and cancelling limit orders are all free transactions.) Specifically, the market order cost c

would have to appear in the stopping regions/impulse controls of the DPEs. The presumed effect would be widening the upper bound on $\delta^{\pm}$ from $1/\kappa$ to $1/\kappa + c$. This would also presumably decrease the overall incidence of market order executions by the strategies.

Discrete posting depths in increments of 1 tick. Presently, the posting depths $\delta^{\pm}$ are continuous variables, and for example in Figure 4.2 were seen to be between 0 and $0.01. In reality, one can only post orders in depth increments of 1 tick, which for the majority of stocks is equal to $0.01. Thus, the current results would have us post at illegal depths. This can partially be solved by rounding the results to the nearest cent, but those rounded depths would no longer have the support of the mathematical derivations, and would likely result in a marked decrease in revenue.

Short term price impact. In order to realize the $2 million profit, we would be executing orders in sizes of 100 shares at a time. In the case of `AAPL` this would have us trading 600k-700k shares per day. `AAPL` has an average daily trading volume of 50m shares, thus we would be contributing more than 1% of daily volume. It is very likely that due to the large quantity of shares we would be transacting each day, our trading would have an impact on the stock price, which generally has an adverse effect on PnL. Modelling this price impact would be an essential component of either generating more realistic returns, or reducing our daily number of trades.

Accounting for non-homogeneity. Currently the calibration method uses entire trading days to determine the value function H and the posting depths $\delta^{\pm}$, which themselves are applied over the whole trading day. However, we saw in the cross-validation section that there are strong grounds for rejecting the time-homogeneity assumption in the underlying data. A feasible extension would be to have independent calibrations for the first hour of trading, last hour of trading, and mid-day trading, as the three are known to have very distinct behaviours.

Backtesting engine: tracking LOB queue position. The backtesting engine that has been used to compute the results uses the $e^{-\kappa\delta}$ limit order fill probability assumption that was made in the stochastic optimal control chapter. Largely, this is because we do not presently track our position in the limit order book queue, and this provides a workaround with some empirical credence. Thus, at present, random numbers effectively

determine whether our limit orders get filled, and in particular, a depth of $\delta = 0$ implies guaranteed execution. However, as we have the ability to reconstruct the entire limit order book from the ITCH data, we thus have all the data we need to actually track our position in the queue, and know with certain whether our order would have been partially or fully executed. Additionally, it's currently implicit that at every timestep we cancel our existing order and repost, even if at the same depth; queue-tracking would force us to make this explicit, adding the option of modifying or keeping our existing orders from the previous timestep.

Backtesting engine: latency. The backtesting engine allows for immediate execution of market orders and posting of limit orders, which ignores the time that a signal takes to be sent from the trading system to the exchange server. As was mentioned in the introduction, minimizing latency is a critical consideration in high-frequency algorithmic trading, and is the justification for the large co-location expenses. Thus it is also paramount to account for its existence in the backtesting engine. A simple 2-5ms lag in execution would realistically simulate the time taken to learn of an event, generate a response, and have the exchange act on the response (Hasbrouck and Saar, 2013).

Early cut-off with optimal liquidation. As was noted in the stochastic optimal control sections, it is never optimal to wait until maturity and pay the liquidation penalty ϕ per share - thus market orders were executed in bulk immediately prior with no penalty. An alternative would be to determine an early cut-off time, on the order of minutes, at which the wealth maximization strategy is ended, and proceed to the end of the day with an optimal liquidation/acquisition strategy.

Bibliography

Almgren, R. and Chriss, N. (2001). Optimal execution of portfolio transactions. *Journal of Risk*, 3:5–40.

Bak, P., Paczuski, M., and Shubik, M. (1997). Price variations in a stock market with many agents. *Physica A: Statistical Mechanics and its Applications*, 246(3):430–453.

Bensoussan, A. (2008). Impulse control in discrete time. *Georgian Mathematical Journal*, 15(3):439–454.

Bertsimas, D. and Lo, A. W. (1998). Optimal control of execution costs. *Journal of Financial Markets*, 1(1):1–50.

Booth, A. (2015). *Automated Algorithmic Trading: Machine Learning and Agent-Based Modelling in Complex Adaptive Financial Markets*. PhD thesis, University of Southampton.

Cartea, Á. and Jaimungal, S. (2013). Modelling asset prices for algorithmic and high-frequency trading. *Applied Mathematical Finance*, 20(6):512–547.

Cartea, Á. and Jaimungal, S. (2015). Incorporating order-flow into optimal execution. *Available at SSRN 2557457*.

Cartea, Á., Jaimungal, S., and Penalva, J. (2015). *Algorithmic and High-Frequency Trading*. Cambridge University Press.

Cartea, Á., Jaimungal, S., and Ricci, J. (2014). Buy low, sell high: A high frequency trading perspective. *SIAM Journal on Financial Mathematics*, 5(1):415–444.

Coleman, T. and Jarrow, R. A. (1998). Cs522 computational tools and methods for finance. Lecture Notes, Cornell University, Department of Computer Science.

Cont, R., Stoikov, S., and Talreja, R. (2010). A stochastic model for order book dynamics. *Operations Research*, 58(3):549–563.

Gosavi, A. (2009). Reinforcement learning: A tutorial survey and recent advances. *INFORMS Journal on Computing*, 21(2):178–192.

Gould, M. D., Porter, M. A., Williams, S., McDonald, M., Fenn, D. J., and Howison, S. D. (2013). Limit order books. *Quantitative Finance*, 13(11):1709–1742.

Guilbaud, F. and Pham, H. (2013). Optimal high-frequency trading with limit and market orders. *Quantitative Finance*, 13(1):79–94.

Hasbrouck, J. and Saar, G. (2013). Low-latency trading. *Journal of Financial Markets*, 16(4):646–679.

Inamura, Y. (2006). Estimating continuous time transition matrices from discretely observed data. Technical report, Bank of Japan.

Kurtz, T. (2004). Mat833 martingale problems and stochastic equations for markov processes. Lecture Notes, University of Wisconsin - Madison, Department of Mathematics.

Kwong, R. (2015). Ece1639 analysis and control of stochastic systems. Lecture Notes, University of Toronto, Department of Electrical & Computer Engineering.

Kyle, A. S. (1989). Informed speculation with imperfect competition. *The Review of Economic Studies*, 56(3):317–355.

Laughlin, G., Aguirre, A., and Grundfest, J. (2014). Information transmission between financial markets in chicago and new york. *Financial Review*, 49(2):283–312.

Lorenz, J. M. (2008). *Optimal trading algorithms: Portfolio transactions, multiperiod portfolio selection, and competitive online search*. PhD thesis, Technische Universität München.

Manyika, J., Chui, M., Brown, B., Bughin, J., Dobbs, R., Roxburgh, C., and Byers, A. H. (2011). Big data: The next frontier for innovation, competition, and productivity. Technical report, McKinsey Global Institute.

Rabiner, L. R. (1989). A tutorial on hidden markov models and selected applications in speech recognition. *Proceedings of the IEEE*, 77(2):257–286.

Rubin, R. and Collins, M. (2015). How an exclusive hedge fund turbocharged its retirement plan. *Bloomberg Business*.

Takahara, G. (2014). Stat455 stochastic processes. Lecture Notes, Queen's University, Department of Mathematics and Statistics.

Tan, B. and Ylmaz, K. (2002). Markov chain test for time dependence and homogeneity: An analytical and empirical evaluation. *European Journal of Operational Research*, 137(3):524–543.

Weißbach, R. and Walter, R. (2010). A likelihood ratio test for stationarity of rating transitions. *Journal of Econometrics*, 155(2):188–194.